European Journal of Taxonomy 836: 131–169
https://doi.org/10.5852/ejt.2022.836.1921
ISSN 2118-9773
www.europeanjournaloftaxonomy.eu
2022 · Tyukosova V. *et al.*

Research article

urn:lsid:zoobank.org:pub:A1C59540-4E3A-405B-ABB1-967D133376CC

Disentangling the identity of *Lebertia porosa* Thor, 1900 using integrative taxonomy (Acari: Hydrachnidia)

Valentina TYUKOSOVA [1], Reinhard GERECKE [2], Elisabeth STUR [3] & Torbjørn EKREM [4,*]

[1,3,4] Department of Natural History, NTNU University Museum, Norwegian University of Science and Technology, NO-7491 Trondheim, Norway.
[2] University of Tübingen, Faculty of Science, Department of Evolution and Ecology, DE-72074 Tübingen, Germany.

[*] Corresponding author: torbjorn.ekrem@ntnu.no
[1] E-mail: v.tyukosova@zoznam.sk
[2] E-mail: reinhard.gerecke@uni-tuebingen.de
[3] E-mail: elisabeth.stur@ntnu.no

[1] urn:lsid:zoobank.org:author:860F3261-36B5-4634-81E2-FCBAA048FAD0
[2] urn:lsid:zoobank.org:author:CB3808B6-9775-4BEF-8FE7-6179AF0DF19F
[3] urn:lsid:zoobank.org:author:30E9790D-32F1-4CB0-97BE-D5F9C3DEA132
[4] urn:lsid:zoobank.org:author:A8E68E2E-405D-4064-9279-27EA493EDA15

Abstract. Initial analyses of DNA barcode data from Norwegian populations attributed to the water mite *Lebertia porosa* Thor, 1900 revealed large genetic divergence and potentially cryptic species-level diversity. We used one mitochondrial (COI) and two nuclear markers (18S and 28S) as well as comparative morphological analysis to redefine *Lebertia porosa*, and to further investigate the species boundaries of Norwegian populations of its close relatives. Our results show that *Lebertia porosa*, as currently defined, consists of multiple species that can be separated by molecular and morphological characteristics. Although we document the presence of the endosymbiotic bacteria *Wolbachia* in two out of eight screened genetic lineages, we find no evidence of intraspecific genetic divergence caused by *Wolbachia* infections. The assignment of one of the genetic lineages to the nominal species could be made through morphological comparisons of specimens from the *L. porosa* type locality with the syntypes of *L. obscura* Thor, 1900. Thus, the diagnosis of *L. porosa* is emended and a neotype is defined. Two of the remaining genetic lineages could be assigned to existing names previously regarded as junior synonyms of *L. porosa*, namely *L. obscura* (lectotype defined here) and *L. gibbosa* Lundblad, 1926, which are both redescribed. The outstanding genetic lineages are unnamed, but from our work we conclude that the taxa *Lebertia porosa britannica* Thor, 1906, *L. porosa dorsalis* Thor, 1906, and *L. porosa italica* Thor, 1906 are nomina dubia that cannot be considered junior synonyms of *L. porosa* as proposed by K. Viets (1956). We also consider *L. vigintimaculata* Thor, 1900 a nomen dubium, probably identical to *L. obscura*.

Keywords. Cryptic species, species delimitation, *Wolbachia*, nomenclature.

Tyukosova V., Gerecke R. Stur E. & Ekrem T. 2022. Disentangling the identity of *Lebertia porosa* Thor, 1900 using integrative taxonomy (Acari: Hydrachnidia). *European Journal of Taxonomy* 836: 131–169. https://doi.org/10.5852/ejt.2022.836.1921

Introduction

The increased use of molecular data to characterize species, and in particular the generation of DNA barcode reference libraries, has revealed cryptic diversity in many arthropod groups (e.g., Hebert *et al.* 2016; Lin *et al.* 2018). While some studies show that large intraspecific genetic divergences are caused by infections of different strains of endosymbiotic bacteria or geographic isolation of different populations (Ferrer-Suay *et al.* 2018), others document that the genetic divergences observed in the barcode marker are corroborated by additional genetic data, morphological characters, and ecology (e.g., Anderson *et al.* 2013; Duarte *et al.* 2019). The use of integrative taxonomy to disentangle the evolutionary entities in species complexes and aggregates is therefore sometimes a prerequisite to generate long-lasting species hypotheses for use in biodiversity research and environmental monitoring.

Several methods have been developed to analyse genetic diversity at the boundary between species, with the goal of creating robust genetic species hypotheses. Each method makes different sets of assumptions and their accuracy changes depending on the studied system (Dellicour & Flot 2018; Puillandre *et al.* 2021). Parameters such as speciation rate, divergence time, population size, interspecific distance, amount of gene flow, etc., are not uniform among organism groups, but can affect the results obtained by various methods (Dellicour & Flot 2018). The conclusions about the best model fits are not transferrable across organism groups with different values for these parameters. Thus, if some of the parameter values are unknown or uncertain, multiple models should be used to verify the delimitation results (Carstens *et al.* 2013). The errors resulting from the model assumptions and assumption violations can manifest themselves in two ways: overestimation or underestimation of the number of operational taxonomic units (OTUs). For instance, the General Mixed Yule Coalescent method (GMYC, Pons *et al.* 2006) is prone to overestimation due to its inability to cope with high, but still biologically plausible, speciation rates (Esselstyn *et al.* 2012; Talavera *et al.* 2013; Dellicour & Flot 2015), while Automatic Barcode Gap Discovery (ABGD, Puillandre *et al.* 2012) and Assemble Species by Automatic Partitioning (ASAP, Puillandre *et al.* 2021), which rely on genetic distances, have some tendency to underestimate the number of OTUs (Pentinsaari *et al.* 2017; Puillandre *et al.* 2021). Bayesian Phylogenetics and Phylogeography (BPP, Yang 2015) and Poisson tree processes (PTP, Zhang *et al.* 2013) assess the posterior probability of species being delimited. The many Markov Chain Monte Carlo (MCMC) iterations run by these models require time and computing power, but despite a small tendency for underestimation in PTP, studies show that the results are often robust and close to the 'true' number of species (e.g., Camargo *et al.* 2012; Pentinsaari *et al.* 2017). However, these methods do not fully account for migration and the results become less accurate in the presence of gene flow between the OTUs, for PTP more so than for BPP (Zhang *et al.* 2011; Luo *et al.* 2018).

The water mite species *Lebertia porosa* Thor, 1900 belongs to the subgenus *Pilolebertia* within the family Lebertiidae Thor, 1900 (Lebertioidea, Hydrachnidia) (Fig. 1). First described by Sig Thor (Sigvart Thorkelsen) from a small stream near the church of Vanse, southern Norway (Thor 1900), the species has a rich taxonomic history with as many as 27 listed junior synonyms (Gerecke 2009). Lundblad already in 1968 defined *L. porosa* as an "eurythermous, Holarctic and probably circumpolar species that lives, however, also far in the South", indicating that this is a generalist with a broad distribution (Lundblad 1968). At the time of its original description in 1900, a total number of 16 species of the genus *Lebertia* had already been named. Among these, due to insufficient diagnostic details and the lack of type material, eight nomina dubia have no relevance today. These include, in addition to the ones listed by K. Viets (Viets 1956: 222–224), also the type species of the genus, *L. tauinsignita* (Lebert,

1879) (Gerecke 2009). Of the remaining nine species, seven are currently accepted: *Lebertia inaequalis* (Koch, 1837), *L. insignis* Neuman, 1880, *L. glabra* Thor, 1897, *L. oudemansi* Koenike, 1898, *L. dubia* Thor, 1899, *L. fimbriata* Thor, 1899, and *L. brevipora* Thor, 1899. One further species has its special nomenclatorial history: *Lebertia vigintimaculata* Thor, 1900 was described in the same publication as *L. porosa*, one page before the latter species. Thus, *L. vigintimaculata* would potentially have priority over *L. porosa*. However, it was later treated as a subspecies of *L. porosa* (*L. porosa vigintimaculata*) by the author himself (Thor 1926), and as its synonym by K. Viets (Viets 1956) (see further discussion below). As evident from the above, the taxonomic history and broad geographical distribution alone make *L. porosa*, in the wide sense, a good candidate for testing species boundaries among morphologically similar populations. In addition, partial cytochrome c oxidase subunit 1 (COI) sequence data (DNA barcodes, Hebert *et al.* 2003) generated through the project 'Water Mites & Midges in Southern Norway' showed strong genetic divergence among specimens originally identified as *L. porosa* (Fig. 2). Given that other species complexes previously have been identified within the Lebertiidae (Pešić *et al.* 2017; Blattner *et al.* 2019), the *L. porosa* aggr. appeared to be a potentially rewarding target for integrative taxonomy.

Congenital bacteria of the genus *Wolbachia* Hertig, 1936 are known to infect many arthropod species. The bacteria maximize their reproductive success by employing multiple strategies such as induced parthenogenesis, male killing, male feminization, and induced cytoplasmic incompatibility between individuals not infected by the same strain (Werren *et al.* 1995, 2008). These strategies may lead to skewed sex ratios or speciation due to forced assortative mating caused by postzygotic reproductive barriers. The presence of multiple strains of *Wolbachia* in a single arthropod species can also result in a pattern of multiple divergent mitochondrial lineages that are discordant with evolutionary lineages in nuclear markers (Whitworth *et al.* 2007; Jiang *et al.* 2018; Sucháčková Bartoňová *et al.* 2021). Although no documented sequence record of *Wolbachia* from Hydrachnidia is available, Blattner *et al.* (2019)

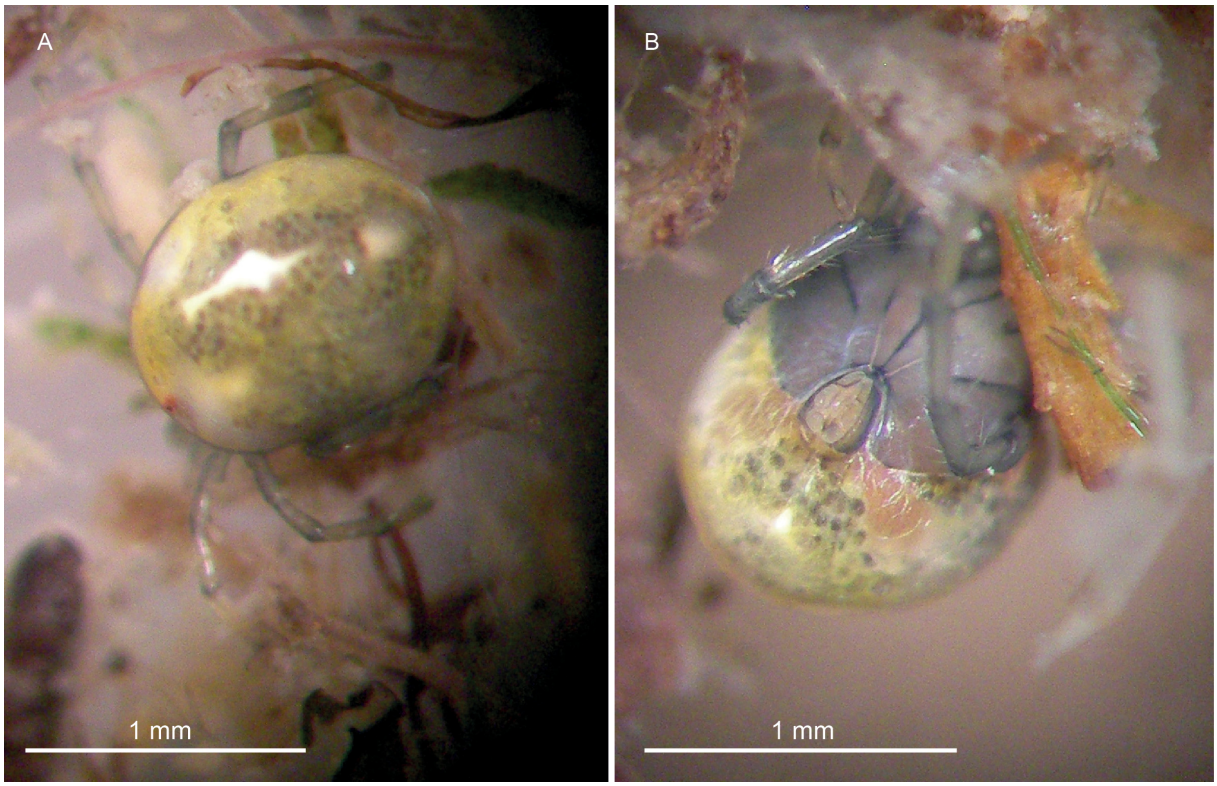

Fig. 1. *Lebertia* (*Pilolebertia*) *porosa* Thor, 1900 s. lat. **A**. Dorsal view. **B**. Ventral view showing acetabula. Photo: Reinhard Gerecke.

Fig. 2. Neighbor Joining tree based on COI barcodes of Norwegian specimens in the *Lebertia porosa* aggr. using the Kimura 2-Parameter substitution model. Bootstrap support (1000 replicates) above 70% is shown on branches.

reported *Wolbachia* infestation in water mites through COI sequences. The sequences, regarded as contamination and therefore discarded, matched with *Wolbachia* or *Rickettsia* da Rocha-Lima, 1916 in NCBI GenBank with 98–100% similarity (Blattner pers comm., May 2022). Moreover, *Wolbachia* has been recorded within other Acari, such as spider mites (Tetranychidae) or predatory mites (Phytoseiidae) (Breeuwer & Jacobs 1996) and infections are also common among the aquatic insect species serving as hosts and prey to water mites (Sazama *et al.* 2017). This could be a potential source of infection, as other mite species have been implicated in horizontal transfer of *Wolbachia* (Cordaux *et al.* 2001; Brown & Lloyd 2015). *Wolbachia* reproduce in a manner similar to cytoplasmic elements and are usually spread vertically by infected females to their offspring. Thus, since the divergent barcode clusters in *L. porosa* are based on the maternally inherited mitochondrial COI marker, the eventual presence and patterns of *Wolbachia* strains infecting the water mites must be assessed.

In this study, we investigate the species boundaries within the *L. porosa* aggr. by analysing both morphological and molecular characters and applying various delimitation methods to mitochondrial and nuclear DNA markers. The main hypothesis of this study is that the genetic clusters observed in the COI data of *L. porosa* aggr. represent multiple morphologically distinct species which are also recognizable as separate genetic lineages in nuclear markers and are not caused by infections with *Wolbachia*. We then use the results to refine the diagnoses and descriptions of species in *Lebertia porosa* aggr. and relate genetically and morphologically separable populations to available names when possible.

Material and methods

Specimens were collected as part of the project 'Water Mites & Midges in Southern Norway' at several localities in South Norway, including the type locality of *Lebertia porosa*. Additional material was also collected during various field trips in Central and North Norway. *Lebertia* (*Lebertia*) sp., used as an outgroup, was collected in a stream near Lake Baikal, Russia. Depending on habitat, kick-sampling, Z-sweeping (where the net is hauled swiftly 2–3 cm over the bottom in a Z-pattern) and small hand-held water net sampling was used to collect substrate that was sorted in white trays in the field. Living mites were collected and fixed in 96% ethanol. Some mites were kept alive for examination and photographic documentation in the laboratory. Thor's material deposited in the Natural History Museum at the University of Oslo (NHMO) was examined for potential syntypes and other references to relevant species. Examined material is deposited in the NTNU University Museum, Norwegian University of Science and Technology, Trondheim, Norway (NTNU-VM); NHMO; Swedish Museum of Natural History, Stockholm, Sweden (NHRS); Senckenberg Research Institute and Natural History Museum, Frankfurt, Germany (SMF), Museum für Naturkunde der Humboldt-Universität Berlin (MNHB), and the Zoological Institute, Russian Academy of Sciences, St. Petersburg, Russia (ZISP). In the taxonomy section, historical material is referred to with exact label information in quotation marks (lines on labels separated by forward slashes).

Morphological analyses

Preparation techniques for water mites have been described and discussed by several authors (Viets 1936; Cook 1974; Smith & Cook 1991). Generally, for the study of the dorsal integument and sclerites of species of *Lebertia*, the idiosoma was dissected with a horizontal cut dorsally from the coxal plate, so that the membranous dorsal integument with lateral eyes and frontal setae was separated from the remainder of the body. The male genital skeleton (morphologically rather uniform among species of *Lebertia*) was separated or left in situ.

The further dissection of *Lebertia* concentrated on the removal of the gnathosoma with the chelicerae, palps, and legs.

Most specimens were mounted for observation in Hoyer's fluid and a few in glycerine jelly. For mounting in Hoyer's fluid, slides were prepared by drying a small drop in the centre at 60°C for 24 hours. For mounting of body parts and appendages, small areas of this drop were re-liquefied to orient the pieces in the boundary layer between the hard and fluid mounting medium. Paired appendages were positioned in a manner that allowed observation of the lateral view of one, and the medial view of the other. Before covering the mounts with a cover slip, slides were again dried for 24 hours. After at least a further 24 hours, the border of the coverslips was sealed with a lacquer ring.

Because nearly all kinds of mounting media have long-term disadvantages (Gerecke 2003), as many specimens as possible were stored undissected after examination in vials.

For the comparative morphological analyses among genetic clades, 54 (25 ♂♂ and 29 ♀♀) slide-mounted specimens were examined using Leica compound microscopes (Leica DM 6000 B or Leica Laborlux K). Measurements were taken using the Leica Application Suite software (Leica Microsystems, Wetzlar, Germany) or by using a calibrated measuring ocular.

The following features were measured: the dorsal length and maximum height of leg and palp segments 2–5, total length and maximum height for leg segment six (Fig. 3A), the length of each acetabulum, the distance between the inner margins of leg four insertions and the length and width of margins one and two on the coxal shield (Fig. 3B), the length of claws on the ultimate leg segments from hinge to tip, from tip to the center of the curvature, and from the center of the curvature to the hinge (Fig. 3C). The numbers and positions of salient setae were noted with emphasis on the number of swimming setae, the distances between the long setae on palp segment 3 (Fig. 3D), and the length and width of the distomedial peg-like seta of palp segment 4. Additionally, the width and length of the gnathosomal bay was measured by creating a line between the openings of the glands at each side and then drawing a perpendicular line from the central fusion seam of the coxal shield (Fig. 3B). In the species analysis, we concentrated on the measurement data providing the most significant results: idiosoma and coxal shield length; Cx-I–II median length; genital flap and Ac length; size and proportions of palp segments and distances of setae on P-3/-4; swimming setae numbers and arrangement; and I-l-4–6 and IV-L-4–6 dimensions and proportions. Measurements are given in µm. Anatomical terminology follows Gerecke (2009).

Abbreviations

I–IV-L-1–6	=	legs I–IV, segments 1–6
Ac-1–3	=	acetabulum 1–3
Cx-I–IV	=	coxae I–IV
dn	=	deutonymph
H	=	height
L	=	length
mL	=	median length
P-1–5	=	palp segments 1–5
upstr.	=	upstream
W	=	width

Specimen IDs starting with HYDCA refer to the specimen IDs used in BOLD. The composition of collected material is given as (males/females/deutonymphs).

Molecular analyses

Fifty specimens distributed among all observed genetic clusters in the Neighbor Joining tree (Fig. 2) from the initial screening were selected for in-depth analyses using additional markers. For some of

the specimens, COI DNA barcode fragments were generated in collaboration with the Norwegian Barcode of Life (NorBOL): DNA extraction on leg tissue, PCR, and bi-directional sequencing followed standard protocols at the Canadian Centre for DNA Barcoding at the University of Guelph, Canada. For the remaining specimens, DNA was isolated non-destructively from whole specimens using Qiagen's DNeasy Blood and Tissue kit (Qiagen) following the manufacturer's instructions for animal tissue samples. Specimens were dried on a piece of filter paper before lysis, and incubation in lysis buffer and proteinase-K was done overnight for approximately 14 hours. DNA was eluted using 100 µl of buffer

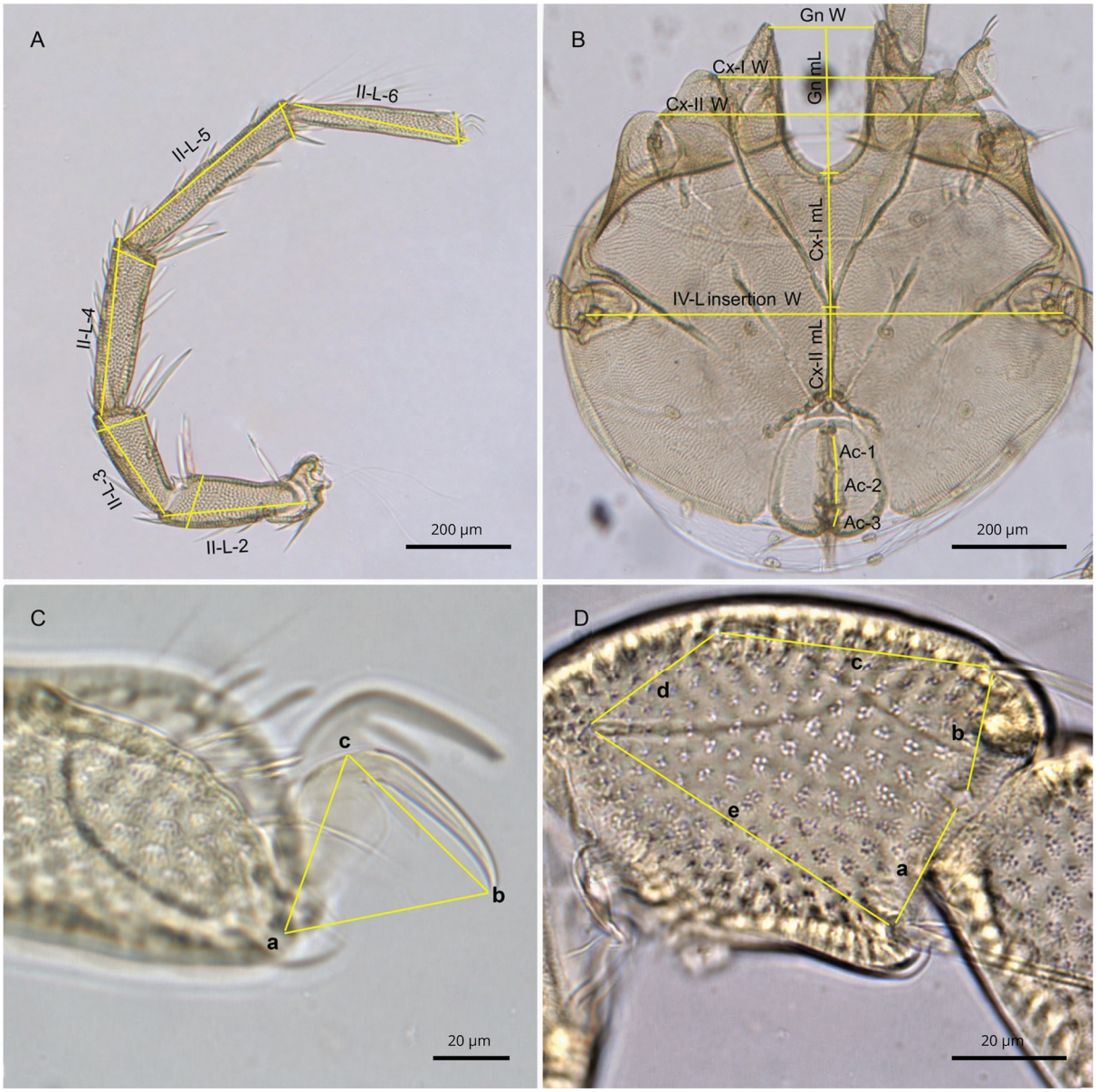

Fig. 3. Genus *Lebertia* Neuman, 1888, positions and shorthand labelling for morphological measurements. **A**. Example of segment length and height measurements for legs and palps. **B**. Measurements across the coxal shield. **C**. The dimensions of the claw; the centre of curvature (c) was defined to be the point opposite of the smaller claw. **D**. Distances among the long setae on the third segment of the palp. Abbreviations: Ac = acetabula; Cx = Coxa; Gn = gnathosomal bay; L = length; mL = median length; W = height; II-L = second leg. Roman numerals refer to the order of legs starting anteriorly, Arabic numerals refer to segment number starting proximally, for Ac starting anteriorly.

AE in the final step. Empty, lysed carcasses were washed in water and 70% ethanol and resuspended in 90% ethanol for later morphological analysis.

PCR amplification of COI, 18S and 28S markers from water mites and the 16S marker from *Wolbachia* used previously published primers (Table 1). PCR reactions in a volume of 20 µl were prepared, consisting of 10 µl of PCR Master Mix 2X (Qiagen), 0.4 µl of 10 µM primer each, and 4 µl of the extracted DNA, with the remaining volume topped up with HyClone Molecular Biology-Grade Water. The PCR cycling conditions for all reactions were: 1 cycle (5 min at 96°C), 35 cycles (30 sec at 95°C, 1 min at 50°C, 1 min at 72°C), 1 cycle (5 min at 72°C) (Dabert *et al.* 2016; Sazama *et al.* 2017). Amplification was verified by electrophoresis on a 1.5% agarose gel. Multiple primers for various *Wolbachia* markers were tested, but all except for 16S DNA (Table 1) failed to amplify under a range of different PCR conditions and annealing temperatures or did not produce readable sequences. For a list of tested *Wolbachia* primers that were unsuccessful see Suppl. File 1. The PCR protocol for *Wolbachia* 16S was the same as for water mite DNA except that 10 µl of Multiplex PCR Master Mix 2X (Qiagen) was used and the annealing temperature was lowered to 45°C. Before sequencing, amplified samples were enzymatically purified with 4 µl of ExoProStar (Cytiva) following the manufacturer's protocol. DNA concentration and purity were checked using a NanoDrop 2000 spectrophotometer (Thermo Scientific) before shipping to Eurofins Genomics for bi-directional Sanger sequencing. All sequences and metadata of sequenced specimens are available in the dataset DS-LPORONOR *Lebertia porosa* s.l. Norway in BOLD (https://doi.org/10.5883/DS-LPORONOR); specimens with NCBI GenBank accessions are listed in Suppl. File 2.

Forward and reverse sequences were examined, aligned, and edited according to their chromatograms using the MEGA X software ver. 10.1.7 (Kumar *et al.* 2018). In some samples, the quality of the forward reading 28S sequence was too low and only the reverse sequence was used for further analysis. The identity of the water mite COI, 28S and 18S fragments were verified using nucleotide Megablast on the NCBI GenBank website (Camacho *et al.* 2009). *Wolbachia* 16S fragments were classified through the Silva database (Quast *et al.* 2013) online version 138.1. The COI sequences were aligned using the BOLD codon aligner (Ratnasingham & Hebert 2007). The 18S and 28S sequences were aligned using the MUSCLE algorithm (Edgar 2004) as available in MEGA X. Gap penalties used were -400 for opening and 0 for extension for 18S and -400 for opening and -200 for extension in 28S. The reliability of the alignments was assessed using GUIDANCE2 (Sela *et al.* 2015). The best substitution model fit was assessed based on the BIC parameter using the 'Find Best DNA/Protein Models (ML)' function in MEGA X and maximum likelihood trees were constructed for each marker with complete gap deletion and 500 bootstrap replicates (Hall 2013). The substitution models used were the TN93+G+I for COI, K2P+G for 18S and T92+G for 28S. The three alignments were concatenated in MEGA X and the 1st, 2nd, and 3rd position partitions in COI, 28S, and 18S were analysed using PartitionFinder ver. 2.1 (Lanfear *et al.* 2017) implementing PhyMl (Guindon *et al.* 2010) and the greedy algorithm (Lanfear *et al.* 2012). A phylogeny of the concatenated dataset was estimated using raxmlGUI ver. 2.0 (Edler *et al.* 2021) implementing RAxML-NG (Kozlov *et al.* 2019) using three partitions (Subset1 = 646-1601, 1-645\3; Subset2 = 2-645\3, 1602-2377; Subset3 = 3-645\3) under the GTR model with gamma distribution of rates across sites and a proportion of invariant sites.

Delimitation and network analysis using multiple molecular delimitation methods were applied to the dataset from each individual marker, excluding sequences from the outgroup and *L. insignis* Neuman, 1880 (the only two taxa that could be morphologically distinguished at the start of the project). A single threshold GMYC was performed in R Studio (ver. 4.0.2) using the Splits package (Ezard *et al.* 2009; R-Core-Team 2020). Ultrametric ML trees for the analysis were prepared in MEGA X using the 'Compute timetree' function. Single marker PTP was performed at https://species.h-its.org/ptp/ using 100 000 MCMC generations and a burn-in of 0.1 (Zhang *et al.* 2013). ABGD and ASAP were performed with the webservices for these tools,

Table 1. Primers used for amplification of DNA fragments.

Primer	Direction	Marker	Sequence (5′–3′)	Original publication
Leb_F	F	COI	CAA ACC AYA AAG AYA TTG GAA C	(Blattner *et al.* 2019)
Leb_R	R		CGA AGA ATC AAA ATA RRT GTT G	
28SHy_F	F	28S	AGT ACC GTG AGG GAA AGT TG	(Blattner *et al.* 2019)
28SHy_R	R		GGC AGG TGA GTT GTT ACA CA	
18Sfw	F	18S	CTT GTC TCA AAG ATT AAG CCA TGC A	(Dabert *et al.* 2010)
rev960	R		GAC GGT CCA AGA ATT TCA C	
Wspecf	F	16S	AGC TTC GAG TGA AAC CAA TTC	(Werren & Windsor 2000)
Wspecr	R		GAA GAT AAT GAC GGT ACT CAC	

https://bioinfo.mnhn.fr/abi/public/abgd/ and https://bioinfo.mnhn.fr/abi/public/asap/, respectively, using the K2P option (Puillandre *et al.* 2021). The command-line version of BPP (A10) using all three markers was run for 500 000 MCMC generations with a burn-in of 0.1 using the COI tree as a guide. The inverse gamma priors for the θ and τ parameters were $\alpha = 3$, $\beta = [0.001, 0.002, 0.01, 0.02]$. Due to the lack of data for the θ and τ parameters for Hydrachnidia, various combinations of the β values were tested for both θ and τ (Yang 2015; Flouri *et al.* 2018). A TCS haplotype network of the COI sequence data was constructed in PopART (Clement *et al.* 2000; Leigh and Bryant 2015).

Results

Gene trees and species delimitation

Good quality mite sequences from COI, 18S, and 28S were obtained from 47 specimens, including 41 specimens fitting the morphological diagnosis of *Lebertia porosa*, five specimens of *L. insignis*, and one specimen of subgenus *Lebertia* (outgroup). Comparison with the type material of *L. obscura* Thor, 1900 and *L. gibbosa* Lundblad, 1926 as well as careful examination of specimens from the type locality of *L. porosa* and *L. obscura* (see below), enabled us to provide valid names for specimens belonging to three of the different genetic clusters in the original COI-tree. The final alignments of the included markers were 645 bp with 228 variable and 213 parsimony informative sites for COI, 776 bp with 53 variable and 42 parsimony informative sites for 18S, and 956 bp with 220 variable and 175 parsimony informative sites for 28S. All sequences were lightly AT biased with the highest average ratio in COI: 64.9% for all positions and 82% for the third codon position.

Phylogenetic analysis of the individual marker alignments showed no conflict between the gene trees (Suppl. File 3: Suppl. Figs 1–3), albeit less genetic divergence between groups was observed for the 18S and 28S markers compared with COI. 18S contained insufficient variation to separate between *Lebertia* aggr. spp. D and E (Suppl. File 3: Suppl. Fig. 2). The ML phylogeny based on the concatenated dataset (Fig. 4) showed strong bootstrap support (100%) for the major genetic groups that were identified in the full NJ COI tree (Fig. 2).

Species delimitation analyses of individual datasets using GMYC, PTP, ASAP, and ABGD separated the *Lebertia porosa* aggr. sequences into 6–19 OTUs depending on method and marker (Table 3). Disregarding the overestimation of 19 OTUs by GMYC for COI and 28S, all methods estimate 6–7 OTUs. For the 28S marker, only GMYC delimits the clades *Lebertia* aggr. sp. D and E as separate OTUs. None of the methods delimit these clades as separate for 18S. GMYC, PTP, ASAP, and ABGD all delimit *Lebertia* aggr. sp. C as two OTUs for at least one marker. For the 18S marker, *Lebertia* aggr. sp. A and B do not show sufficient divergence to be delimited by any of the methods.

The multimarker species delimitation analysis using BPP resulted in seven OTUs among the *L. porosa* clusters, with posterior probability for the entire model ranging from 0.74 to 0.95. The lower posterior probability in the model with more conservative values of θ and τ is mainly the result of a lower posterior probability for the support for the node dividing *Lebertia* aggr. spp. D and E.

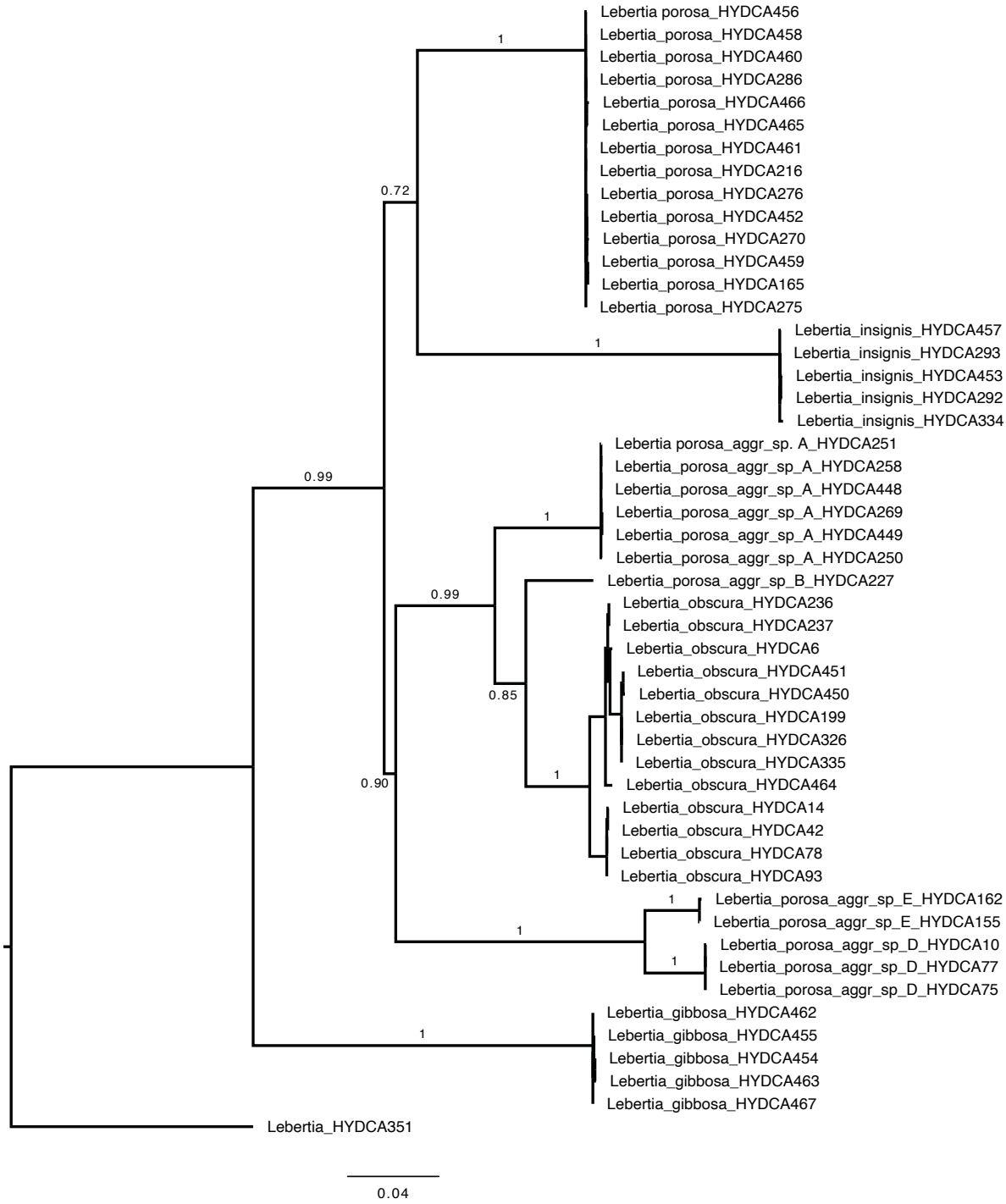

Fig. 4. *Lebertia* (*Pilolebertia*) spp. in Norway. Maximum Likelihood tree from analysis of the concatenated dataset (COI, 18S, 28S) in RAxML-NG. Bootstrap support (500 replicates) above 50% on branches.

The TCS haplotype network of COI sequences clearly separates nine major groups (Fig. 5). Apart from *Lebertia obscura*, the network shows low reticulation with a high number of mutations between nodes.

Wolbachia

All 47 specimens included in the phylogenetic and species delimitation analyses were tested for the presence of *Wolbachia* using the 16S marker and *Wolbachia* specific primers. Seventeen specimens showed positive results from PCR amplification. Three different bacterial fragment lengths were

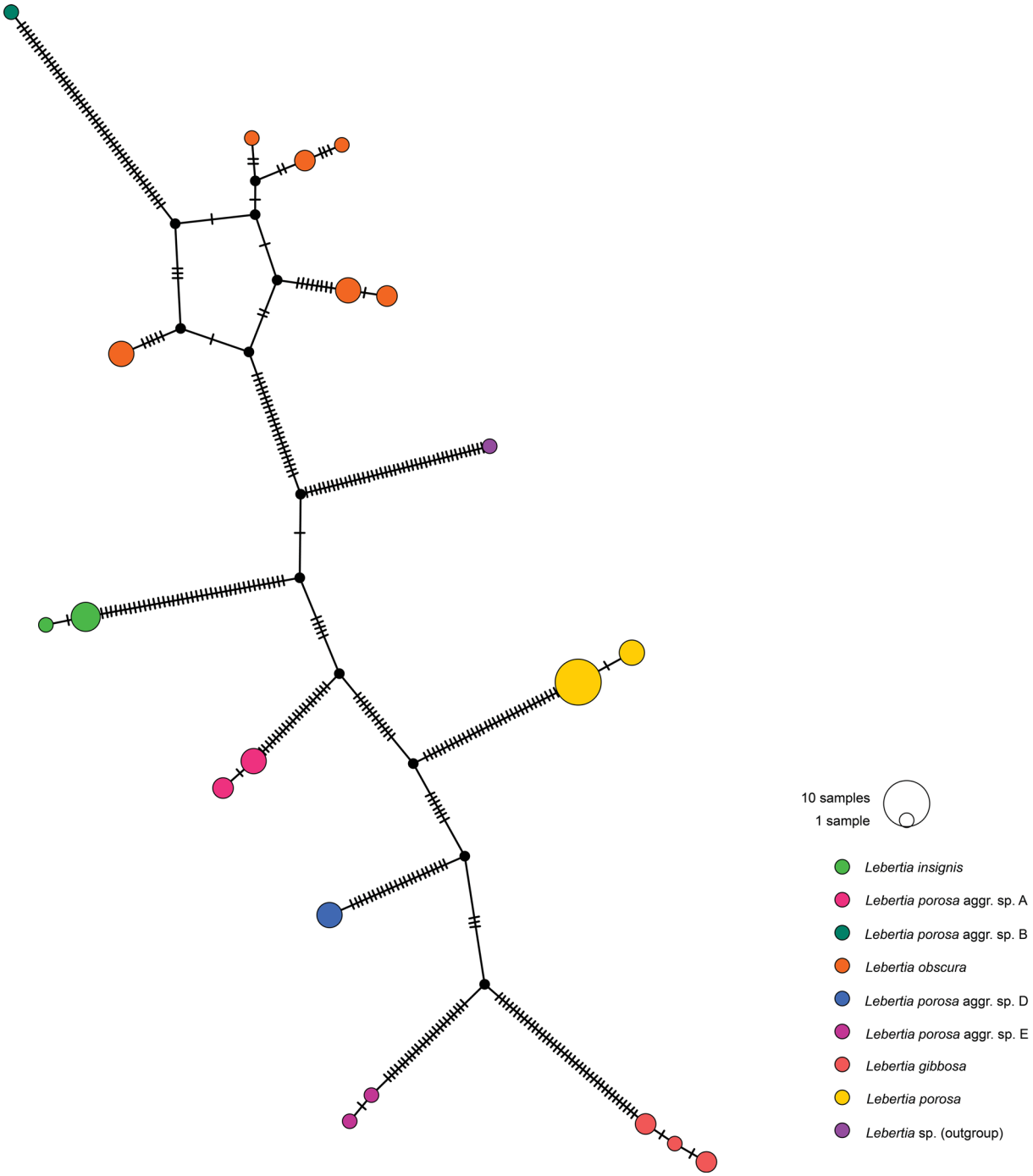

Fig. 5. *Lebertia* (*Pilolebertia*) spp. from Norway. TCS haplotype network of COI sequences constructed with PopART.

Table 2. Results from species delimitation analyses using GMYC, PTP, ASAP, and ABGD on individual marker datasets showing the number of OTUs delimited. Sequences from *Lebertia* (s. str.) sp. (outgroup) and *L. insignis* (the only taxon of *Pilolebertia* that could be morphologically separated at the start of the project) were excluded.

Marker	GMYC	PTP	ASAP	ABGD
COI	19	7	7	7
18S	7	6	6	7
28S	19	6	7	7

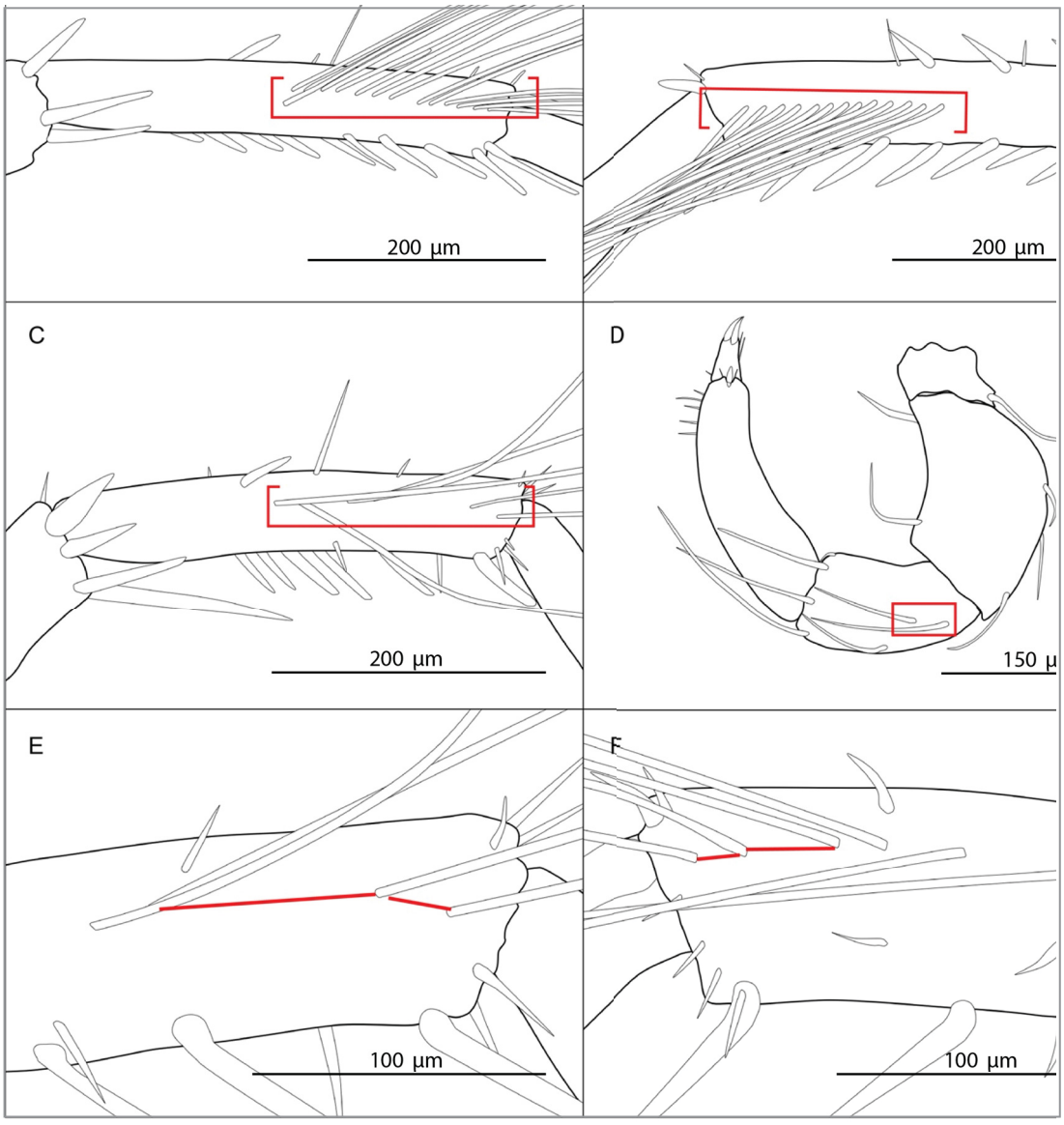

Fig. 6. *Lebertia* (*Pilolebertia*) spp. Examples of observed differences in setation. **A–B**. High number of setae on segment five of legs three and four (III-L-5, IV-L-5) present in *Lebertia* aggr. spp. B and D. **C**. Gap in swimming setae on the fifth segment of the second leg (II-L-5) in *Lebertia* aggr. spp. A and B, and *L. obscura* Thor, 1900. **D**. Segment three of palp (P-3) with a double proximal long seta sometimes present in *Lebertia* aggr. spp. D. **E–F**. Segment five of the second leg (II-L-5), close-up: comparison of swimming setae with and without the large gap respectively.

Table 3. A presence/absence matrix of morphological characteristics observed in *L. porosa* aggr. clades. Characteristics marked with +/- were not present in all examined specimens. Abbreviations: Ac = acetabula, L = length, P = palps, I–IV-L-1–6 = Legs I–IV segments 1–6. Roman numerals refer to the order of legs starting anteriorly. Arabic numerals refer to segment number starting proximally. The exact position for the measurement of P-3 distance d can be found in Fig. 3D.

Character	*L. gibbosa*	*L. obscura*	*L. porosa*	sp. A	sp. B	sp. D	sp. E
	3 ♂♂, 2 ♀♀	5 ♂♂, 7 ♀♀	7 ♂♂, 7 ♀♀	5 ♂♂, 6 ♀♀	2 ♀♀	3 ♂♂, 3 ♀♀	2 ♂♂, 2 ♀♀
II-L-5 large gap in swimming setae		+		+/-	+		
III-L-5 >14 swimming setae					+	+	
IV-L-5 >14 swimming setae					+	+	
P-3 doubled most proximal seta						+/-	
IV-L-4 ≥9 swimming setae						+	+
II-L-5 swimming setae stop before distal edge	+						
III-L-6 Stout (L/H<5)	+		+	+			
IV-L-6 Stout (L/H<5)				+			
P-3 distance D long (L≥38 µm)				+			
I-L slender (I-L-(4-6) L/H>3.2,4.2,4.2)					+		
IV-L slender (I-L-(5-6) L/H>6.0,4.2)		+					
Coxal field long (L>1000 µm)						+	
Palp long and slender (P-3 L>140, P-4 L>195 µm, P-3 L/H>1.85)						+	
Legs long and slender (I-L-(4-6) L>450, 490, 430 µm, L/H>5...)						+	
P-2 relatively short (L P-2/P-3 < 1.2)							+
Genital field with large acetabula (Ac-1 L=85-95 µm)							+
Leg segments short (I-L-(4-6) L=130-145, 138-150, 125-130 µm)	+						
Palp short and slender (P-2 L<110, P-4 L<140 µm, P-3 L/H>2.2)	+						

successfully sequenced: 270 bp, 490 bp and 900 bp. Only the six longest fragments could be positively identified as *Wolbachia* in the Silva database. The highest identity match in the Silva database was 95% and the 10 nearest neighbors included *Wolbachia* extracts from a quill mite (*Torotrogla cardueli* Bochkov & Mironov, 1999), a spider mite (*Bryobia* sp.), a nematode parasitizing ticks (*Cercopithifilaria japonica* Uni, 1983), the giant yellow aphid (*Tuberolachnus salignus* Gmelin, 1790), and a springtail (*Neelus murinus* Folsom, 1896). All the generated sequences were highly similar, presenting only three variable sites and no parsimony informative sites. Of the six identifiable sequences, five originated from the specimens belonging to *Lebertia porosa* (HYDCA216, HYDCA276, HYDCA252, HYDCA258, HYDCA260) and one from *Lebertia obscura* (HYDCA78).

Morphological comparison

Morphological comparative analysis among genetic clades revealed that each possessed a unique combination of characters (Table 3, Fig. 6). The diagnostic features of each clade (i.e., proportions of palp and leg segments, numbers of swimming setae) include character states which are different from those used in the current morphological identification of *L. porosa* (Gerecke 2009).

Taxonomy

Class Arachnida Lamarck, 1801
Order Trombidiformes Reuter, 1909
Suborder Prostigmata Kramer, 1877
Cohort Parasitengona Oudemans, 1909
Superfamily Lebertioidea Thor, 1900
Family Lebertiidae Thor, 1900
Genus *Lebertia* Neuman, 1888
Subgenus *Pilolebertia* Thor, 1900

Lebertia* (*Pilolebertia*) *porosa Thor, 1900
Fig. 7

Lebertia (*Pilolebertia*) *porosa* Thor, 1900: 273, pl. 10 figs 3–4.

Diagnosis

Palp relatively large (L P-2 > 120, P-4 > 150). P-3 stout (L/H ratio < 2.1), with position of mediodistal seta rather variable (often halfway between, occasionally approaching the dorso- or ventrodistal one). P-4 ventral sectors between seta insertions decreasing in length from base to tip (in % total L: proximal sector 42–49, central sector 33–38, distal sector 15–22). I-L rather long (L I-L-4–6 > 170, 180, 160), IV-L-4–6 relatively stout (L/H ratio < 4.1, 5.2, 4.6), terminal claw L > 70.

Type series

Missing. Type locality: Norway, "Lister, Flusz nahe bei Vanse Kirche"; no date, no information on number of specimens (at least one male).

Material examined

Neotype (here designated)
NORWAY • ♂; Agder, Farsund, Vanse, stream at Vanse school; 58.10366° N, 6.69373° E; 6 m a.s.l.; 25 Jun. 2020; Torbjørn Ekrem and Thomas Stur Ekrem leg.; kick sample; BOLD specimen ID HYDCA568 (in ethanol); NTNU-VM 227972.

Further material from type locality

NORWAY • 3 ♂♂; same collection data as for neotype; BOLD specimen ID HYDCA436 (in ethanol), HYDCA438 (slide mounted), HYDCA465 (in ethanol); NTNU-VM 228032, 228034, 228036 • 3 ♀♀; same collection data as for neotype; BOLD specimen HYDCA437 (in ethanol), HYDCA439 (slide mounted), HYDCA466 (in ethanol); NTNU-VM 228033, 228035, 228037 • 1 ♂; same collection data as for neotype; in ethanol; NTNU-VM 228040 • 2 ♀♀; same collection data as for neotype; in ethanol; NTNU-VM 228039, 228041 • 3 ♀♀; same collection data as for neotype; in ethanol; NTNU-VM 228042 • 1 ♂; same collection data as for neotype; stream at playground; 58.09846° N, 6.69490° E; BOLD specimen ID HYDCA570 (slide mounted); NTNU-VM 228043.

Other material (in ethanol unless otherwise stated)

NORWAY • 2 ♂♂, 2 ♀♀, 2 dn; "*Lebertia porosa* Sig Thor 22-7-1899 Selsvand, Gudbr.dal. Sig Thor"; NHMO • 1 ♂; "*Lebertia (Pilolebertia) porosa* S. Thor / 3-8-1899. Baverdal, Raubergstaltjern Sig Thor"; NHMO • 1 ♂, 9 ♀♀; "*L. porosa* Sig Thor", "*Lebertia* / 6-8-1898 Bekk ved Norbö [undecipherable] Jaderen Sig Thor"; NHMO • 1 ♂, 2 ♀♀; "*Leb. (Pilolebertia) porosa* Sig Thor (+ ? ind.) [meaning unclear, vial was broken] 18/7.1899 Hattendal , Fjelstjörn v. Hatten Nordland" [no collector, possibly coll. E. Strand, see Thor 1900b]; NHMO • 4 ♀♀; "*Lebertia ? porosa* Sig Thor / 24-7-1898, Baek nor Herikstad (Aagland) Jaederen / Teknes Sig Thor; NHMO • 1 ♀; "Pil. porosa S.T.", "*Lebertia* n. sp. NB (epimerora) [indecipherable] / 5-10-1900 Ljanselv. Sig Thor"; NHMO • 4 ♂♂, 2 ♀♀; "*L. (Pilolebertia) porosa* Sig Thor (ikke rev.) / 17-7-1896 Himesjö nær Aamot, Österdalen, Norge leg. Sig Thor"; NHMO • 2 ♀♀; "*Lebertia (Pilolebertia) ? porosa* Sig Thor / 13-7-1897, Landöelv, Senjen Dr. Sig Thor"; NHMO • 2 ♀♀; "*Leb. (Piloleb.) porosa* Sig Thor ? var. / 19-7-1897 Stor vandet (Hammerfest) ½ aq. + ½ v.l. Sig Thor"; NHMO • 6 ♂♂, 3 ♀♀, 1 dn; "*Lebertia (Piloleb.) porosa* Sig Thor. / 26-7-1897, Tsoalmejarve, Syd-Varang. Finnmarken N. Sig Thor"; NHMO • 2 ♂♂, 2 ♀♀; "*Lebertia (Pilol.) ? porosa* Sig Thor / 29-8-1900, Balsokvand, Balsfjord Nordm."; NHMO • 1 ♀; "*Lebertia porosa* sp.n. Sig Thor / 22-7-1900. Elv ved Alteid (Tromsöand) Sig Thor"; NHMO • 3 ♂♂; "*Lebertia (Piloleb.) porosa* Sig Thor. 16/8 1899 Raubergstult. / 16-8-1899 Raubergstultjern Baverdal, Gudbr.dal, Sig Thor"; NHMO • 1 ♀; "*Leb*. (*Pilolebertia*) cfr. *porosa* ST. / 14-7-1898 Kittelsav i Torrisdal n. sten og mos paa bunden ST"; slide mounted; NHMO • 1 ♂; "*Lebertia insignis* Neum. ♂ Cotype. / Norwegen. Hjatdala [!] Hjartdal. 29.7.1901 S. Thor leg. 2001"; SMF 44901 • 1 ♂; "*Lebertia insignis* Neum. ♂ Cotype. S. Thor 1900 / Norwegen. Selsvand, Gudbrandsdal 22.7.1899 Thor leg. 2005"; slide mounted; SMF 44902 • 1 ♀; "*Lebertia insignis* Neum. ♀ Cotype / Norwegen. Selsvand, 7.1899 Thor leg. 2006"; slide mounted; SMF 44903 • 1 ♀; "*Lebertia* (*Piloleb*.) *porosa* var. Sig. Thor Cotype ♀ / Norwegen Larvik, Farris-elv. 2.11.1913. S. Thor leg. et det. 1691"; slide mounted; SMF 45001 • 1 ♂; "*Lebertia* (*Piloleb*.) *porosa* var. Sig. Thor Cotype ♂ / Norwegen Larvik, Farris-elv. 2.11.1913. S. Thor leg. et det. 1693"; slide mounted; SMF 45002 • 1 ♂; Agder, Flekkefjord, Flikkeid, creek at Flikkeid 18; 58.35775° N, 6.62518° E; 56 m a.s.l.; 24 Aug. 2019; Gaute Kjærstad and Reinhard Gerecke leg.; BOLD specimen ID HYDCA556; NTNU-VM 227997 • 2 ♂♂, 1 dn; same collection data as for preceding; NTNU-VM 227998, 227999 • 1 ♂; Agder, Froland, inlet stream to Horvedalstjenn, upstream bridge, intersection Lyngrothveien; 58.52377° N, 8.67591° E; 53 m a.s.l.; 28 Aug. 2019; Gaute Kjærstad and Reinhard Gerecke leg.; BOLD specimen ID HYDCA312; NTNU-VM 228004 • 1 ♂; Agder, Flekkefjord, Lundevatn at Sira, Sirneset; 58.40630° N, 6.62017° E; 48 m a.s.l.; 24 Aug. 2019; Gaute Kjærstad and Reinhard Gerecke leg.; slide mounted; NTNU-VM 228000 • 1 ♀; Agder, Kristiansand, creek at bridge close to Nedre Timenes vei nr. 51; 58.16324° N, 8.10116° E; 1 m a.s.l.; 27 Aug. 2019; Gaute Kjærstad and Reinhard Gerecke leg.; drift sample; BOLD specimen ID HYDCA270 (slide mounted); NTNU-VM 228001 • 1 ♂; Agder, Kristiansand, Kvernbekken, at Kjos; 58.11431° N, 7.95185° E; 1 m a.s.l.; 27 Aug. 2019; Gaute Kjærstad and Reinhard Gerecke leg.; BOLD specimen ID HYDCA275 (slide mounted); NTNU-VM 228002 • 1 ♀; same collection data as for preceding; BOLD specimen ID HYDCA276 (slide mounted); NTNU-VM 228003 • 1 ♀; Agder, Kristiansand, Prestebekken, close to Jegersberg gård; 58.16420° N, 8.00735° E; 4 m a.s.l.; 2 Sep. 2019; Reinhard Gerecke and Torbjørn Ekrem leg.; BOLD specimen ID HYDCA340;

NTNU-VM 228029 • 2 ♀♀, 1 dn; same collection data as for preceding; NTNU-VM 228030 • 1 ♂; Agder, Kristiansand, Nedre Jegersbergvann, inlet flow stream; 58.16920° N, 8.00007° E; 21 m a.s.l.; 2 Sep. 2019; Reinhard Gerecke and Torbjørn Ekrem leg.; BOLD specimen ID HYDCA560; NTNU-VM 228028 • 1 ♀; Agder, Lillesand, Badstudalen nature reserve, creek in Eigedalen; 58.20614° N, 8.23545° E; 43 m a.s.l.; 22 Jun. 2020; Gaute Kjærstad leg.; BOLD specimen ID HYDCA566; NTNU-VM 228031 • 1 ♂, 2 ♀♀; Agder, Songdalen, Stavbekken, at Dynamitten; 58.15848° N, 7.81138° E; 45 m a.s.l; 30 Aug. 2019; Gaute Kjærstad and Reinhard Gerecke leg.; BOLD specimen ID HYDCA425 (slide mounted), HYDCA426 (slide mounted), HYDCA452; NTNU-VM 228008, 228009, 228010 • 3 ♂♂, 2 ♀♀; same collection data as for preceding; NTNU-VM 228011–228013 (slide mounted), 228014; • 2 ♂♂, 1 ♀; Agder, Søgne, Søgneelva, upstream bridge close to old Søgne Church; 58.08952° N, 7.83998° E; 2 m a.s.l.; 30 Aug. 2019; Gaute Kjærstad and Reinhard Gerecke leg.; BOLD specimen ID HYDCA286 (slide mounted), HYDCA460, HYDCA461; NTNU-VM 228005, 228016, 228017 • 1 ♂, 2 ♀♀; same collection data as for preceding; NTNU-VM 228006, 228007, 228018 • 1 ♂; same locality as for preceding; 21 Jun. 2020; Gaute Kjærstad leg.; BOLD specimen ID HYDCA435 (slide mounted); NTNU-VM 228015 • 5 ♀♀; same collection data as for preceding; NTNU-VM 228019 • 3 ♂♂, 3 ♀♀; Agder, Søgne, Søgneelva, Ved Fossheia; 58.09047° N, 7.83637° E; 3 m a.s.l.; 30 Aug. 2019; Gaute Kjærstad and Reinhard Gerecke leg.; BOLD specimen ID HYDCA294, HYDCA295, HYDCA430, HYDCA431, HYDCA458, HYDCA459; NTNU-VM 228020 to 228025 • 3 ♂♂, 1 ♀; same collection data as for preceding; NTNU-VM 228026, 228027 • 1 ♂; Møre og Romsdal, Eide, Nåsvassdraget, Sagelva, station 1; 62.89968° N, 7.42313° E; 8 m a.s.l.; 14 Sep. 2016; Gaute Kjærstad leg.; BOLD specimen ID HYDCA216 (slide mounted); NTNU-VM 228050 • 1 ♀; same collection data as for preceding; NTNU-VM 228051 • 1 ♂; Telemark, Drangedal, Engåa, creek; 59.03875° N, 9.28733° E; 71 m a.s.l.; 17 Jun. 2020; Gaute Kjærstad leg.; BOLD specimen ID HYDCA369 (slide mounted); NTNU-VM 227992 • 1 ♀; same collection data as for preceding; BOLD specimen ID HYDCA370 (slide mounted); NTNU-VM 227993 • 4 ♀♀; same collection data as for preceding; NTNU-VM 227994 to 117996 • 1 ♀; Trøndelag, Meråker, Stjørdalsvassdraget, Stjørdalselva, station 6; 63.44283° N, 11.62808° E; 92 m a.s.l.; 26 Apr. 2016; Gaute Kjærstad leg.; BOLD specimen ID HYDCA538; NTNU-VM 228047 • 2 ♀♀; Trøndelag, Stjørdal, Stjørdalselva at Hegra; 63.46305° N, 11.08623° E; 4 m a.s.l.; 3 Jul. 2020; Valentina Tyukosová and Torbjørn Ekrem leg.; BOLD specimen ID HYDCA456, HYDCA572; NTNU-VM 228044, 228045 • 1 ♀; Trøndelag, Stjørdal, Stjørdalsvassdraget, Stjørdalselva, station 1; 63.46251° N, 11.09256° E; 33 m a.s.l.; 26 Apr. 2016; Gaute Kjærstad leg.; BOLD specimen ID HYDCA537; NTNU-VM 228046 • 1 ♂; Trøndelag, Stjørdal, Stjørdalsvassdraget, Stjørdalselva, station 8; 63.41707° N, 11.73635° E; 99 m a.s.l.; 30 Aug. 2018; Gaute Kjærstad leg.; BOLD specimen ID HYDCA165 (slide mounted); NTNU-VM 228048 • 1 ♀; same collection data as for preceding; NTNU-VM 228049.

SWEDEN • 1 ♀; "granskad av Thor 1925 / *Pilolebertia porosa* Sig Thor. ♀ var. Jytland: Linding Aa vid Varde. Vid inloppet i Nörholm Skov. Vattentemp. + 14°C, kl. 7 c.m. Leg. J.K. Findal. 15.6.1928. 428."; NHRS GULI000086301.

Description

Idiosoma colouration pale brown with an irregular yellowish median line surrounded by a darker area, lateral eye pigment red, appendages pale brown. Integument smooth, with a very fine porosity, in some specimens after enzymatic digestion a very fine striation becomes visible. Coxal field with mL Cx-I > Cx-II (ratio 1.1–1.3). Posterior margin of Cx-IV equally rounded or, in aged adults, only weakly convex in part facing V-3, posteromedial part turning in an abrupt curve to genital bay. Genital bay with nearly straight, anteriorly converging lateral margins and obtuse anterolateral angles at level of pregenital sclerite. Genital flaps with sexual dimorphism in setation, anterior and central Ac elongate, posterior Ac roundish.

Legs rather long, but distal segments of hind leg stout. Swimming setation: II-L-5 6–7; III-L-4 5–7; III-L-5 4–12; IV-L-4 5–10; IV-L-5 9–12.

Gnathosoma (lateral view) ventral margin in basal part equally convex, in distal part straight or very weakly concave, without a kink near mouth opening area. Chelicera slender as typical in most *Lebertia*, with short claw (L/H ratio 6.4–7.4, basal segment/claw ratio 4.5–5.4). Palp relatively stout; P-2 dorsal margin more strongly curved in basal part than distally, ventral margin equally concave, with a slight protrusion at base of ventral seta, 5–6 dorsal setae; P-3 stout, dorsal and ventral margins only slightly diverging from base to tip, with five setae: one proximomedial and one dorsocentral, three medially at distal margin, typically at equal distance (mediodistal seta halfway between dorsodistal and ventrodistal one), but mediodistal setae may approach one of the two others. P-4 maximum H in proximal quarter, from here towards tip of segment equally narrowed; fine ventral setae dividing ventral segment margin into three sectors of unequal size, with proximal one largest and distal one shortest, but distoventral seta always further away from distoventral edge than its insertion point from dorsal margin; mediodistal peg setae strong and blunt, dorsally 6–8 fine setae, all restricted to a small groove in distalmost part of segment.

Males

Idiosoma L 1000–1320; coxal shield L 750–830; Cx-I/II mL 210–220/170–180. Genital field L/W 150–205/160–175; L Ac-1 70–75, L Ac-2 55–70, L Ac-3 40–50; genital flaps with ca 50 pairs of setae at medial margin, arranged in a single line on level of Ac-1, in a double line near Ac-2, and in triple line near Ac-3.

Leg measurements (L/H, ratio): I-L-4 169–195/59–73, 2.73–2.96; I-L-5 187–205/48–58, 3.48–3.91; I-L-6 161–180/42–50, 3.50–3.95; IV-L-4 290–313/75–80, 3.63–4.12; IV-L-5 310–534/57–68, 4.90–5.42; IV-L-6 279–315/57–75, 4.20–5.11; proportions of segments (L ratio): IV-L-4/5 0.90–0.96, IV-L-4/6 0.97–1.06, IV-L-5/6 1.08–1.12; IV-L claw L 75–85.

Palp measurements (L/H, ratio, % total L): P-1 40–43/58–60, 0.7, 8%; P-2 125–143/81–95, 1.46–1.70, 27–28%; P-3 99–123/58–68, 1.61–1.85, 23–24%; P-4 147–163/46–53, 2.92–3.20, 31%; P-5 49–50/9, 5.56–5.74, 9–10%; proportions of segments (L ratio): P-2/P-3 1.14–1.40, P-2/P-4 0.84–0.91, P-3/P-4 0.64–0.73; distance ratio distal setae P-3 (A/B) 0.69–1.38; P-4 ventral sectors 42–53%, 29–36%, 18-22%; dorsal/ventral L ratio 1.16–1.22; palp total L 513–516.

Females

Idiosoma L 1200–1300; coxal shield L 820–830; Cx-I/II mL 205–230/175–185. Genital field L/W 220–230/175–190; L Ac-1 70, L Ac-2 60–65, L Ac-3 50–55; genital flaps with ca 20 pairs of setae in a single line at medial margin.

Leg measurements (L/H, ratio): I-L-4 183–202/64–73, 2.74–3.03; I-L-5 198–216/53–60, 3.58–3.88; I-L-6 176–198/45–55, 3.45–4.00; IV-L-4 308–345/77–90, 3.74–4.25; IV-L-5 319–375/64–73, 4.86–5.33; IV-L-6 319–340/68–80, 4.00–4.74; proportions of segments (L ratio): IV-L-4/5 0.91–0.97, IV-L-4/6 0.97–1.07, IV-L-5/6 1.06–1.12; IV-L claw L 80–85.

Palp measurements (L/H, ratio, % total L): P-1 38–40/58–59, 0.65–0.68, 8%; P-2 132–150/88–97, 1.49–1.62, 28%; P-3 95–128/57–73, 1.65–1.83, 24%; P-4 155–174/51–59, 2.91–3.21, 32%; P-5 50–53/9, 5.56–5.83, 9–11%; proportions of segments (L ratio): P-2/P-3 1.13–1.40, P-2/P-4 0.78–0.89, P-3/P-4 0.68–0.74; distance ratio distal setae P-3 (A/B) 0.50–1.00; P-4 ventral sectors 47–48%, 33–38%, 15–19%; dorsal/ventral L ratio 1.18; palp total L 500–539.

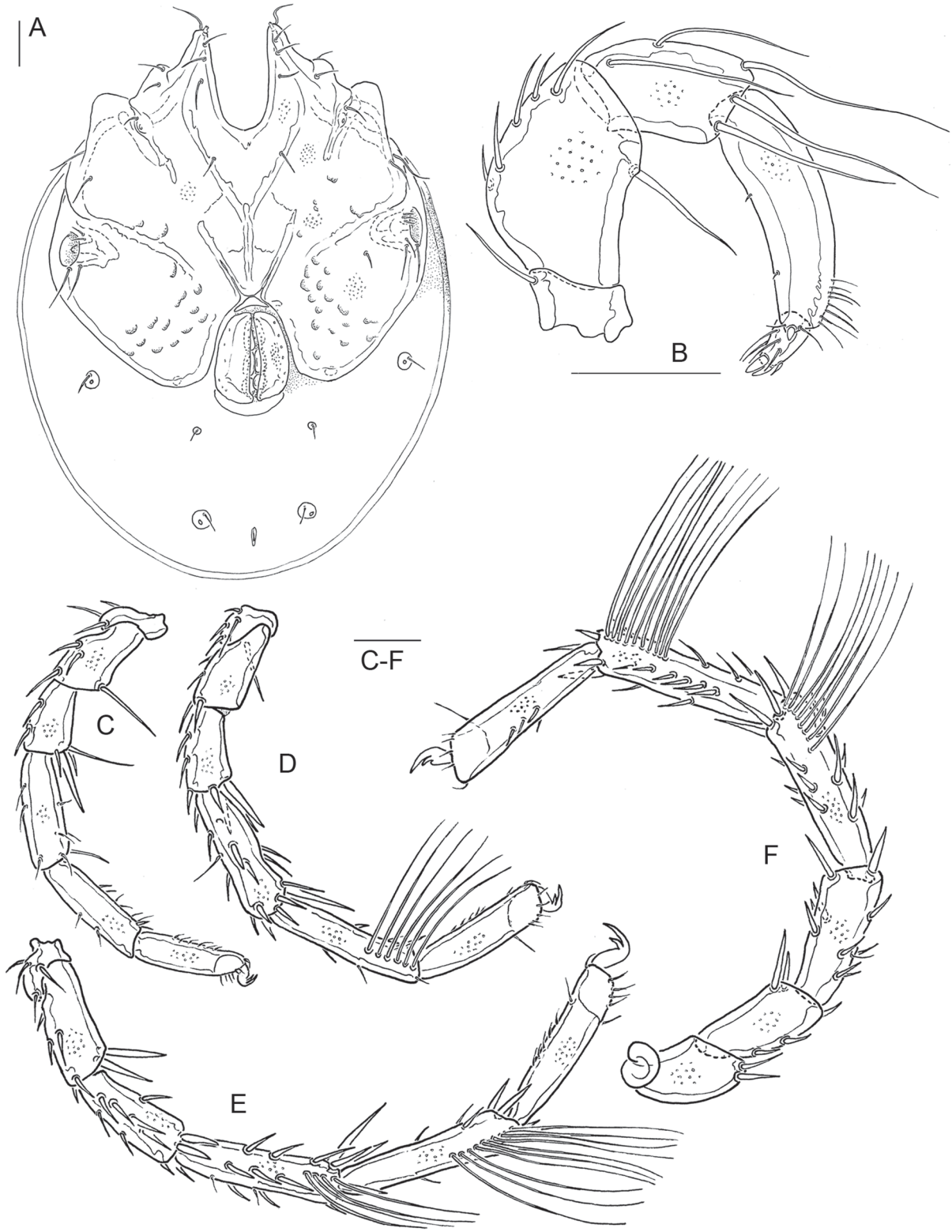

Fig. 7. *Lebertia* (*Pilolebertia*) *porosa* Thor, 1900, ♂ from the type locality. **A**. Venter. **B**. Palp. **C**. I-L. **D**. II-L. **E**. III-L. **F**. IV-L. Scale bars = 100 µm.

Remarks

In the original description, Thor (1900: pl. 10 figs 3–4) included a reference to two figures, but he later (Thor 1906) stated that these figures show *L. porosa obscura*. Thus, no figure in the original description is ascribed to *L. porosa*. Characters considered diagnostic by Thor was the body colouration (idiosoma dark brown with yellow dorsal line) and the formation of the integument (thick, densely covered by name-giving fine pores – these pores "stronger and more apparent than in *L. insignis* and *L. vigintimaculata*"). The described fine, line-like folds in the integument were later considered artifacts (Thor 1902). A lineation as it is typical in many species of other subgenera has not yet been found in any species of *Pilolebertia*. Further characters given in the original description are as follows: idiosoma L/W 1400/1200–1300; palps and legs very thick; legs with rich swimming setation; coxal field as in *L. insignis*/*vigintimaculata*, but suture Cx-III/IV directed "a bit more laterally"; Cx-IV occasionally with a small indentation "within the large pore" (probable meaning: posterior margin of Cx-IV in the part facing V-3 slightly flattened or concave, as given by Thor (1900: fig. 3) for *L. obscura*). No taxonomic significance can be attributed to differences in porosity patterns of the integument of species of *Pilolebertia*, density and size of pores most probably being age dependent.

At the time of its description, the species had to be distinguished from two other species of the subgenus *Pilolebertia*: *Lebertia inaequalis* Koch, 1837, which could be separated by having both ventral setal pores of P-4 in the distal part of the segment, the distal one very close to the distal segment edge, peg seta of P-4 very small, not longer than high, and by having a gnathosomal ventral margin with a kink near the mouth opening; and *L. insignis* Neuman, 1880, which could be separated by having the distomedial seta on P-3 very close to the distoventral one, ratio 0.29–0.33. The latter species is similar to *L. porosa* and differs from *L. inaequalis* in having the gnathosoma without a distal kink and in the rather large distomedial peg seta on P-4. Our data reveal that *L. insignis* can be distinguished from both compared species also by the insertion of the ventral setae on P-4, with the central sector longer than both the proximal and distal sectors. This species is also unique in having the proximal and distal sectors nearly equal in size (L ratio 0.84–1.07; in most other genetic lineages the proximal sector is relatively enlarged, L ratio > 1.1).

Redefining *Lebertia porosa* after material collected at its type locality was more complicated than expected, as representatives of three distinct genetic clades were detected at the same site, all with *porosa*-like character combinations following Gerecke (2009). Two findings helped us to attribute one of these clades to *L. porosa*: (1) one of the three clades could be clearly distinguished from *L. porosa* on the basis of morphological features (most probably, this taxon had already been found by Thor in Norway as well, but not at this site; it represents *L. gibbosa* Lundblad, 1926, see below); (2) syntypes of *L. obscura* found at NHMO could be attributed to the second of these clades. Through an elimination process it was thus possible to attribute the third clade from the Vanse locality to *L. porosa*.

The indication "Cotype" on the labels of specimens of *Lebertia insignis* and *L. porosa* in SMF (see above) are obviously incorrect, but all the specimens in question (SMF 44901–44903 and 45001–45002) are in good agreement with the definition given for *L. porosa*.

During the first quarter of the past century, nine *porosa*-like species of *Lebertia* were described, all listed as junior synonyms (Gerecke 2009): *Lebertia pachydermis* Koenike, 1908; *L. lacertosa* Koenike, 1911; *L. saxonica* Thor, 1911; *L. seclusa* Koenike, 1914; *L. rivalis* Koenike, 1918; *L. violacea* K. Viets, 1921; *L. violacea lurida* K. Viets, 1921; *L. leioderma* K. Viets, 1925; *L. porosa curvata* K. Viets, 1925. The type material of *L. saxonica* has not been found. For all other species, types could be investigated for comparison with the material included in our study here. For several of these species, a synonymy with *L. porosa* or *L. obscura* is probable. For others, a revival or their designation as nomina dubia is possible. Comparative studies to clarify this are ongoing and it is too early to present results, but the

character states of all these species are distinctly different from the character combination diagnostic for *L. gibbosa*. Hence, there is no doubt about the taxonomic stability of the latter.

Lebertia riabuschinskii Thor, 1926 was listed by Gerecke (2009) as a synonym of *L. porosa*, erroneously referring to Besseling (1958). Lundblad (1956) and later authors proposed to synonymize *L. riabuschinskii* with *L. inaequalis*. In fact, data kindly made available by A. Shatrov on material conservated at ZISP confirm that material attributed to *L. riabuschinskii* (no type material exists) is morphologically close to *L. inaequalis*. The same is true for two specimens from Finland in SMF, labelled as *L. riabuschinskii*. This species will be treated in a projected revision of the *L. inaequalis* group.

Before this revision, *L. porosa* was considered a eurytopic and euryoecious species with a Holarctic distribution (Gerecke 2009). Our results show that both distribution and ecology need to be revised on a broader scale for accuracy, taking into account that populations in other regions likely represent species other than *L. porosa*. At present the 'true' *Lebertia porosa* is recorded from middle order streams at low altitudes (up to 220 m a.s.l.) in Norway and Sweden only, but in a wide range of geographical latitudes from Agder in the south (58° N) to Finnmark in the north (69° N).

Lebertia* (*Pilolebertia*) *obscura Thor, 1900
Fig. 8

Lebertia (*Pilolebertia*) *porosa obscura* Thor, 1900: 273.

Diagnosis

Palp relatively large (L P-2≥130, P-4≥150). P-3 stout (L/H<1.9), with position of mediodistal seta rather variable (often halfway between, occasionally approaching the dorso- or ventrodistal one). P-4 ventral sectors between seta insertions various, in many cases decreasing in length from base to tip (in % total L: proximal sector 35–55, central sector 22–45, distal sector 17–27). I-L rather long (L I-L-4–6>165, 185, 160), IV-L-4–6 relatively slender (L/H ratio>4.1, 5.9, 4.7); terminal claw L<60.

Type series

Type locality: Norway, "Lister, Flusz nahe bei Vanse Kirche"; no date, no information on number of specimens, at least one male.

Material examined

Lectotype (here designated)
NORWAY • ♂; "20-7-98 Elv fra Prest ved Vanse (Listerland) Sig Thor / *Lebertia* ? n. sp. *obscura*" [Agder, Farsund, Lister, Vanse, stream at Vanse vicarage]; 58.10366° N, 6.69373° E; 6 m a.s.l.; 20 Jul. 1898; Sig Thor leg.; in ethanol; one II-L, one IV-L detached; NHMO.

Paralectotypes
NORWAY • 1 ♀; same collection data as for lectotype; NHMO • 2 ♀♀; "*Lebertia porosa* ST + *obscura* Sig Thor / 20-7-1898. Elv pa Vanse, Lister, Sig Thor"; slide mounted; NHMO.

Other material (in ethanol unless otherwise stated)
NORWAY • 3 ♂♂, 3 ♀♀; "*Lebertia porosa* ST + var. *obscura* Sig Thor / 13-8-1901. Elv ved Vanse, Lister, Sig Thor"; slide mounted; NHMO • 4 ♂♂, 11 ♀♀; "17-8-1901. Slavdalsvand, Lister. Sig Thor / *Lebertia porosa* S.T. v. *obscura* S.T."; of these, 2 ♂♂ and 2 ♀♀ slide mounted; NHMO • 3 ♀♀; same collection data as for preceding, "Thymol"; NHMO • 1 ♂; same collection data as for preceding; "*Lebertia obscura*"; NHMO • 1 ♀; "K. Viets 45040", "*Lebertia porosa obscura* S. Thor Cotype / Norwegen Lister

17.8.1901 S. Thor leg. 2004"; slide mounted; SMF • 1 ♀; Agder, Farsund, Vanse, stream at Vanse school [type locality]; 58.10366° N, 6.69373° E; 6 m a.s.l.; 25 Jun. 2020; Torbjørn Ekrem and Thomas Stur Ekrem leg.; kick sample; BOLD specimen ID HYDCA464; NTNU-VM 227971 • 1 ♀; Agder, Farsund, Vanse, stream at playground; 58.09846° N, 6.69490° E; 6 m a.s.l.; 25 Jun. 2020; Torbjørn Ekrem and Thomas Stur Ekrem leg.; kick sample; BOLD specimen ID HYDCA571; NTNU-VM 227973 • 1 ♂, 1 ♀; Agder, Flekkefjord, Lake Lundevatn at Sira, Sirneset; 58.40630° N, 6.62017° E; 48 m a.s.l.; 24 Aug. 2019; Gaute Kjærstad and Reinhard Gerecke leg.; BOLD specimen ID HYDCA442, HYDCA443; NTNU-VM 227961, 227962 • 2 ♀♀; same locality as for preceding; slide mounted; NTNU-VM 227963, 227964 • 2 ♂♂, 1 ♀; Agder, Kristiansand, Foss, Jordfallbekken, downstream at bridge; 58.26850° N, 8.16259° E; 26 m a.s.l.; 26 Aug. 2019; Gaute Kjærstad and Reinhard Gerecke leg.; BOLD specimen ID HYDCA236, HYDCA237, HYDCA278 (all slide mounted); NTNU-VM 227966, 227967, 227965 • 4 ♀♀; same locality as for preceding; NTNU-VM 227978 • 1 ♂, 1 ♀; Agder, Kristiansand, Songdalen, creek close to Oxbow Lake at Bruhaugen; 58.15623° N, 7.82584° E; 12 m a.s.l.; 21 Jun. 2020; Gaute Kjærstad leg.; BOLD specimen ID HYDCA564, HYDCA565; NTNU-VM 227968, 227969 • 2 ♂♂; same locality as for preceding; slide mounted; NTNU-VM 227980 • 1 ♂; Agder, Kristiansand, Søgne, Flomdam, Søgneelva, upstream of the bridge at old Søgne church; 58.08962° N, 7.83937° E; 2 m a.s.l.; 30 Aug. 2019; Gaute Kjærstad and Reinhard Gerecke leg.; NTNU-VM 227979 • 1 ♀; Agder, Lillesand, Badstudalen nature reserve, Fanturheia; 58.20626° N, 8.23249° E; 45 m a.s.l.; 22 Jun. 2020; Gaute Kjærstad leg.; BOLD specimen ID HYDCA567; NTNU-VM 227970 • 2 ♀♀, 4 dn; Agder, Lillesand, Badstudalen nature reserve, stream in Eigedalen; 58.20614° N, 8.23545° E; 43 m a.s.l.; 22 Jun. 2020; Gaute Kjærstad leg.; NTNU-VM 227981 • 1 dn; Nordland, Vefsn, Drevvatnet, station 3; 66.048° N, 13.387° E; 47 m a.s.l.; 10 Jun. 2013; Gaute Kjærstad leg.; BOLD specimen ID HYDCA42 (slide mounted); NTNU-VM 227943 • 2 ♀♀; Nordland, Vefsn, Drevvatnet, station 1; 66.052° N, 13.364° E; 47 m a.s.l.; 11 Aug. 2014; Gaute Kjærstad leg.; BOLD specimen ID HYDCA17, HYDCA78 (both slide mounted); NTNU-VM 227944, 227945 • 1 ♂; Nordland, Vefsn, Drevjavassdraget, Drevvatnet, station 2; 66.0674° N, 13.416° E; 47 m a.s.l.; 9 Aug. 2016; Gaute Kjærstad leg.; BOLD specimen ID HYDCA180 (slide mounted); NTNU-VM 227975 • 4 ♀♀, 1 ♂; Nordland, Vefsn, Fustvatnet, station 1; 65.907° N, 13.361° E; 38 m a.s.l.; 13 Aug. 2014; Gaute Kjærstad leg.; BOLD specimen ID HYDCA6, HYDCA9, HYDCA90, HYDCA91, HYDCA93 (all slide mounted); NTNU-VM 227946 to 227950 • 1 ♀; Nordland, Vefsn, Fustvatnet, station 3; 65.906° N, 13.432° E; 38 m a.s.l.; 13 Aug. 2014; Gaute Kjærstad leg.; BOLD specimen ID HYDCA14 (slide mounted); NTNU-VM 227951 • 1 ♂; Nordland, Vefsn, Fusta vassdraget, Fustvatnet, station 3; 65.9061° N, 13.432° E; 38 m a.s.l.; 11 Aug. 2016; Gaute Kjærstad leg.; BOLD specimen ID HYDCA175 (slide mounted); NTNU-VM 227974 • 1 ♂, 2 ♀♀; Telemark, Drangedal, Engåa (pool); 59.03855° N, 9.28759° E; 71 m a.s.l.; 17 Jun. 2020; Gaute Kjærstad leg.; BOLD specimen ID HYDCA335, HYDCA367, HYDCA368 (all slide mounted); NTNU-VM 227952 to 227954 • 1 ♀; same locality as for preceding; NTNU-VM 227976 • 3 ♂♂, 1 ♀; Telemark, Drangedal, Krossbekken, at gate; 59.04808° N, 8.70406° E; 464 m a.s.l.; 20 Aug. 2019; Gaute Kjærstad leg.; BOLD specimen ID HYDCA326 (slide mounted), HYDCA327, HYDCA450, HYDCA451; NTNU-VM 227955 to 227958 • 17 ♂♂, 7 ♀♀; same locality as for preceding; of these, 2 ♂♂ slide mounted; NTNU-VM 227977, 227959, 227960 • 1 ♂; Trøndelag, Orkdal, Orklavassdraget, Sagbekken, station 1; 63.24614° N, 9.67573° E; 175 m a.s.l.; 26 Jul. 2018; Gaute Kjærstad leg.; BOLD specimen ID HYDCA199; NTNU-VM 227990 • 2 ♂♂, 1 ♀; Trøndelag, Stjørdal, Stjørdalsvassdraget, Stjørdalselva, station 8; 63.41707° N, 11.73635° E; 99 m a.s.l.; 30 Aug. 2018; Gaute Kjærstad leg.; NTNU-VM 227988, 227989 • 6 ♂♂, 6 ♀♀, 2 dn; Trøndelag, Stjørdal, Hegra, opposite of gas station at E14; 63.4631° N, 11.0853° E; 71 m a.s.l.; 3 Jul. 2020; Torbjørn Ekrem and Valentina Tyukosová leg.; NTNU-VM 227982 to 227989.

Description

In good agreement with the description given above for *L. porosa* (corresponding details not repeated here). Colouration of appendages dark blue green. Coxal field with mL Cx-I > Cx-II (ratio 1.1 : 1.7). Legs

rather long, distal segments of hind leg relatively slender. Swimming setation: II-L-5 2–9; III-L-4 6–10; III-L-5 8–14; IV-L-4 6–9; IV-L-5 7–12. Chelicera L/H ratio 7.3–7.8, basal segment/claw ratio 5.8–8.1.

Males

Idiosoma L 1220–1400; coxal shield L 780–950; Cx-I/II mL 210–280/150–190. Genital field L/W 200–250/200–210; L Ac-1 64–75, L Ac-2 57–70, L Ac-3 35–45; genital flaps with ca 40 pairs of setae at medial margin, arranged in a single line on level of Ac-1–2, in double and triple lines near Ac-3.

Leg measurements (L/H, ratio): I-L-4 167–200/59–70, 2.77–2.96; I-L-5 187–223/48–58, 3.71–4.10; I-L-6 160–180/40–48, 3.68–4.00; IV-L-4 304–400/65–85, 4.18–5.11; IV-L-5 330–430/51–70, 6.00–7.00; IV-L-6 293–344/48–60, 6.00–6.17; proportions of segments (L ratio): IV-L-4/5 0.92–0.94, IV-L-4/6 1.03–1.13, IV-L-5/6 1.09–1.22; IV-L claw L 45–50.

Palp measurements (L/H, ratio, % total L): P-1 35–43/54–70, 0.61–0.65, 7–8%; P-2 130–175/78–100, 1.50–1.68, 27–29%; P-3 95–130/62–75, 1.54–1.73, 22%; P-4 150–193/50–59, 2.96–3.28, 33–34%; P-5

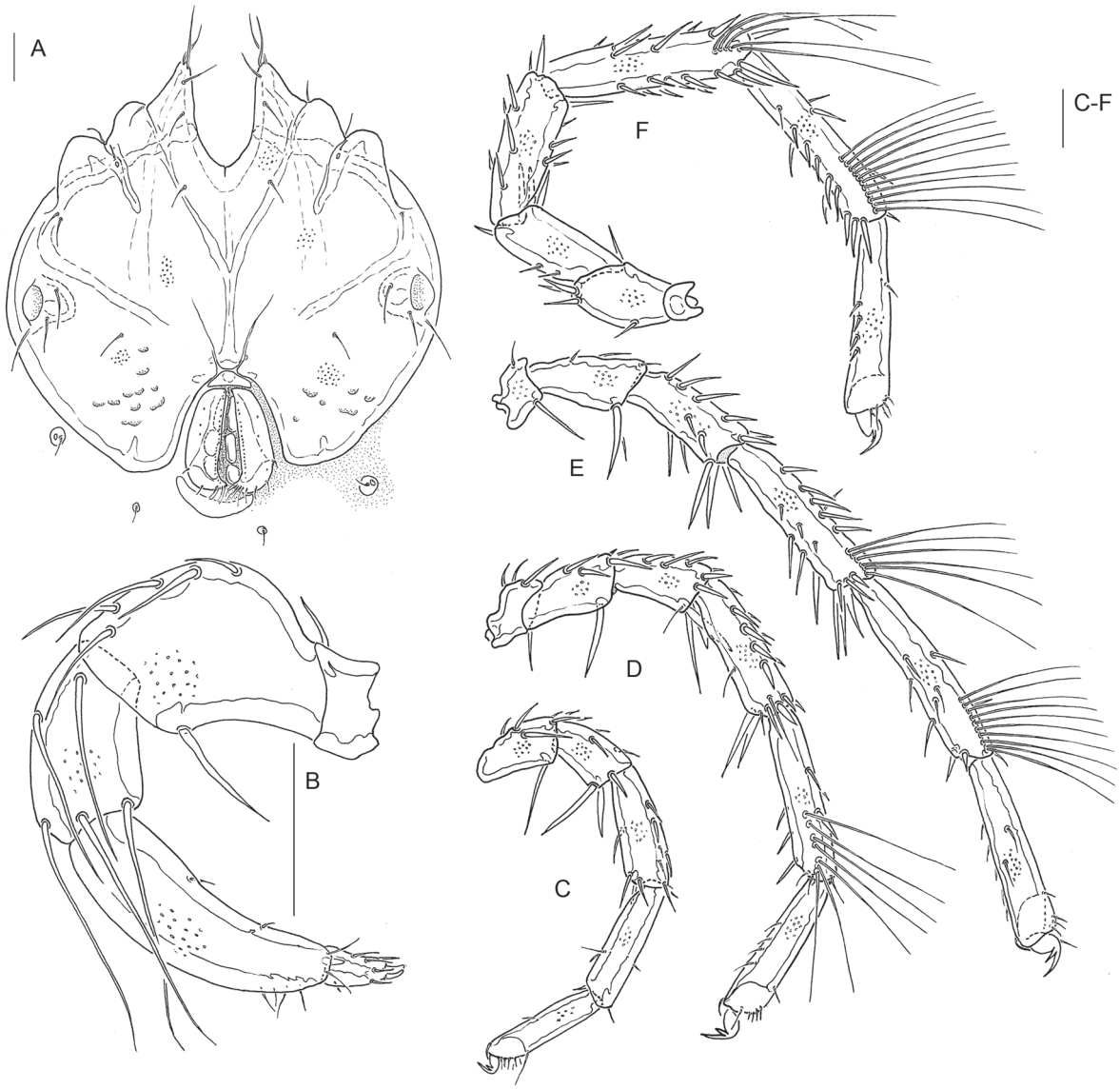

Fig. 8. *Lebertia* (*Pilolebertia*) *obscura* Thor, 1900, ♂ from the type locality. **A**. Coxal field. **B**. Palp. **C**. I-L. **D**. II-L. **E**. III-L. **F**. IV-L. Scale bars = 100 μm.

45–55/8–10, 5.50–6.25, 9–10%; proportions of segments (L ratio): P-2/P-3 1.22–1.40, P-2/P-4 0.80–1.00, P-3/P-4 0.63–0.71; distance ratio distal setae P-3 (A/B) 0.68–1.71; P-4 ventral sectors 37–55%, 22–45%, 17–22%; dorsal/ventral L ratio 1.18–1.23; palp total L 465–588.

Females

Idiosoma L 1050–1600; coxal field L 850–1050; Cx-I/II mL 215–280/160–190. Genital field L/W 210–290/190–230; L Ac-1 75–85, L Ac-2 65–80, L Ac-3 50–65; genital flaps with ca 25 pairs of setae at medial margin, arranged in a single line.

Leg measurements (L/H, ratio): I-L-4 187–211/64–75, 2.82–2.93; I-L-5 200–231/51–59, 3.64–4.09; I-L-6 165–180/44–51, 3.61–4.00; IV-L-4 341–400/66–81, 4.67–5.17; IV-L-5 352–444/55–64, 6.00–7.00; IV-L-6 304–363/52–65, 4.77–6.31; proportions of segments (L ratio): IV-L-4/5 0.89–0.97, IV-L-4/6 1.06–1.13, IV-L-5/6 1.16–1.22; IV-L claw L 43–55.

Palp measurements (L/H, ratio, % total L): P-1 33–40/63, 0.52–0.64, 6–7%; P-2 145–180/88–105, 1.49–1.65, 29%; P-3 110–145/66–79, 1.54–1.80, 22%; P-4 165–195/55–70, 2.75–3.08, 32–33%; P-5 50–53/8–10, 5.25–6.25, 9–10%; proportions of segments (L ratio): P-2/P-3 1.22–1.34, P-2/P-4 0.86–0.92, P-3/P-4 0.65–0.74; distance ratio distal setae P-3 (A/B) 0.92–1.40; P-4 ventral sectors 37–55%, 34–38%, 17–27%; dorsal/ventral L ratio 1.17–1.19; palp total L 534–540.

Remarks

The name *obscura* was introduced as a "nov. var." within the description of *L. porosa* for *porosa*-like specimens with dark blue green appendages (Thor 1900: 273). Two figures (Thor 1900: pl. 10 figs 3–4) show the venter of a male and a palp of a specimen of uncertain sex; no further diagnostic features were given by the author.

Lebertia obscura agrees with *L. porosa* in most morphological details, such as the shape of the coxal field, the swimming setation of legs, or the proportions of the palp segments and arrangement of their setae. The most striking difference is found in the formation of the hind leg segments, where *L. porosa* has distinctly stouter segments and longer claws. In addition to the difference in colouration (as highlighted in the original description, *L. porosa* with pale brown, not blue green appendages), our data also show that *L. porosa* has a higher number of setae along the medial margins of the genital flaps.

The designation of the specimen SMF 45040 as a "Cotype" is obviously erroneous (collected after the publishing date of the original description), but it fits the description given here except for the presence of seven strong ventral setae on IV-L-6. In other specimens, the number of these setae does not exceed five, and they are smaller in size. We cannot exclude that Thor was able to distinguish *L. obscura* from *L. porosa* on the base of colouration; the alteration of colours following the fixation of all available material does not allow consideration of this character at present. Among the eight specimens collected at the type locality on 20 Jul. 1898 and 13 Aug. 1901 and labelled "*Lebertia porosa* + *obscura*" by Sig Thor, none agrees with the diagnosis given above for *L. porosa*: seven show character combinations typical for *L. obscura*, and one male is similar to specimens defined as *Lebertia porosa* aggr. sp. A in our investigation, a species which is intermediate between *L. porosa* and *L. obscura* in IV-L proportions (see below).

Our data show a wide distribution of the species in Norway from the far south to Nordland County (65° N). In light of the new species characteristics described here, further research is needed to clarify the geographical distribution of *L. obscura*.

Lebertia* (*Pilolebertia*) *gibbosa Lundblad, 1926
Fig. 9

Lebertia gibbosa Lundblad, 1926: 206.

Diagnosis

Small in dimensions of appendages (e.g., palp total L<420, L IV-L-4–6<260, 290, 260); P-2 short (L 90–105), dorsal margin protruding to form a hump-like edge near insertion of dorsal setae, distoventral seta long (about 110). P-3 (L/H 2.2–2.4) and P-4 (L/H 3.0–3.7) very slender, L ratio P-2/P-3 0.9–1.0, P-3/P-4 0.8–0.9. Mediodistal seta P-3 away from dorsodistal seta (L ratio sectors A/B 1.7–1.8). Ventral seta of P-4 in distal part, distoventral one close to distoventral segment edge (L ventral sectors 57–67, 24–34, 8–9%).

Material examined

Holotype
SWEDEN • ♂, "923. Typ (360) *Lebertia gibbosa* Lundbl. ♂. Östergötland: Kisa rocken. Vålens tillopp. 28.06.1917, leg. O. Lundblad"; slide mounted; NHRS.

Other material (in ethanol unless otherwise stated)
NORWAY • 1 ♂; Agder, Farsund, Vanse, stream at Vanse school; 58.10366° N, 6.69373° E; 6 m a.s.l.; 25 Jun. 2020; Torbjørn Ekrem and Thomas Stur Ekrem leg.; kick sample; BOLD specimen ID HYDCA467; NTNU-VM 227896 • 1 ♂; Agder, Farsund, Vanse, stream at playground; 58.09846° N, 6.69490° E; 6 m a.s.l.; 25 Jun. 2020; Torbjørn Ekrem and Thomas Stur Ekrem leg.; kick sample; BOLD specimen ID HYDCA569; NTNU-VM 227897 • 1 ♂, 2 ♀♀, 1 dn; Agder, Froland, Nidelva, near Blakstad, upstream bridge Frolandsveien, E riverbank; 58.51004° N, 8.64806° E; 40 m a.s.l.; 28 Aug. 2019; Gaute Kjærstad and Reinhard Gerecke leg.; BOLD specimen ID HYDCA306, HYDCA 429, HYDCA454, HYDCA455; NTNU-VM 227882 to 227885 • 2 ♂♂, 2 ♀♀; Agder, Søgne, Søgneelva, upstream bridge close to old Søgne Church; 58.08952° N, 7.83998° E; 2 m a.s.l.; 21 Jun. 2020; Gaute Kjærstad and Reinhard Gerecke leg.; BOLD specimen ID HYDCA432 (slide mounted), HYDCA433 (slide mounted), HYDCA 462, HYDCA463; NTNU-VM 227886 to 227889 • 1 ♂, 2 ♀♀; same collection data as for preceding; slide mounted; NTNU-VM 227891 to 227893 • 2 ♂♂, 2 ♀♀; same locality as for preceding; 30 Aug. 2019; NTNU-VM 227890 • 1 ♂; Agder, Søgne, Flomdam, Søgneelva upstream bridge near old Søgne church; 58.08962° N, 7.83937° E; 2 m a.s.l.; 30 Aug. 2019; Gaute Kjærstad and Reinhard Gerecke leg.; BOLD specimen ID HYDCA558; NTNU-VM 227894 • 1 ♂; same collection data as for preceding; NTNU-VM 227895 • 1 ♀, 1 dn; Trøndelag, Orkdal, Orklavassdraget, Sagbekken, station 1; 63.24614° N, 9.67573° E; 175 m a.s.l.; 26 Jul. 2018; Gaute Kjærstad leg.; NTNU-VM 227998.

Description

Colour in life unknown. Integument with a fine porosity. Coxal field with medial sutures Cx-I slightly longer than medial sutures Cx-II (ratio about 1.2), Cx-II posteromedially forming a narrow, acute angle. Posterior margin of Cx-IV equally rounded or forming an obtuse angle near apodeme in medial sector. Swimming setation: II-L-5 4–5; III-L-4 4–5; III-L-5 7–9; IV-L-4 4–5; IV-L-5 7–9. Chelicera L/H ratio 8.0, basal segment/claw ratio 7.0.

Males
Idiosoma L 1060, coxal shield 740, Cx-I/II mL 190/165. Genital field L/W 190/130, with 34–44 medial setae; Ac-1–3 L 65, 50, 35. Gnathosoma L 200; chelicera basal segment L 270, H 55; claw 60.

Leg measurements (L/H, ratio): I-L-4 121–132/46–48, 2.62–2.86; I-L-5 125–138/37–40, 3.35–3.65; I-L-6 99–125/35–38, 2.81–3.35; IV-L-4 227–240/48–55, 4.36–4.86; IV-L-5 242–260/37–43, 6.12–6.47;

IV-L-6 207–225/40, 5.22–5.63; proportions of segments (L ratio): IV-L-4/5 0.92–0.94, IV-L-4/6 1.07–1.10, IV-L-5/6 1.15–1.17; IV-L claw L 50.

Palp measurements (L/H, ratio, % total L): P-1 30/43, 0.7, 8; P-2 92–96/60–62, 1.5–1.6, 25; P-3 97–103/44–45, 2.2–2.3, 27; P-4 112–123/36–38, 3.1–3.3, 32; P-5 33/5, 7,2, 8; proportions of segments (L ratio): P-2/P-3 0.94–0.96, P-2/P-4 0.79–0.82, P-3/P-4 0.83–0.86; distance ratio distal setae P-3 (A/B) 1.67; P-4 ventral sectors 63%, 28%, 9%; palp total L 384.

Females

Idiosoma L 900–1200; coxal shield 720–750; Cx-I/II mL 210–225/170. Genital field L/W 180–190/150, with 18–24 medial setae; Ac-1–3 L 55–60, 55–60, 38–40. Gnathosoma L 210; chelicera basal segment L 210, H 30; claw 30.

Leg measurements (L/H, ratio): I-L-4 145/50, 2.90; I-L-5 150/40, 3.75; I-L-6 130/38, 3.47; IV-L-4 255/60–65, 3.92–4.25; IV-L-5 273–280/48–55, 4.95–5.89; IV-L-6 240–250/43–45, 5.33–5.88; proportions of segments (L ratio): IV-L-4/5 0.91–0.94, IV-L-4/6 1.02–1.06, IV-L-5/6 1.12–1.14; IV-L claw L 50–55.

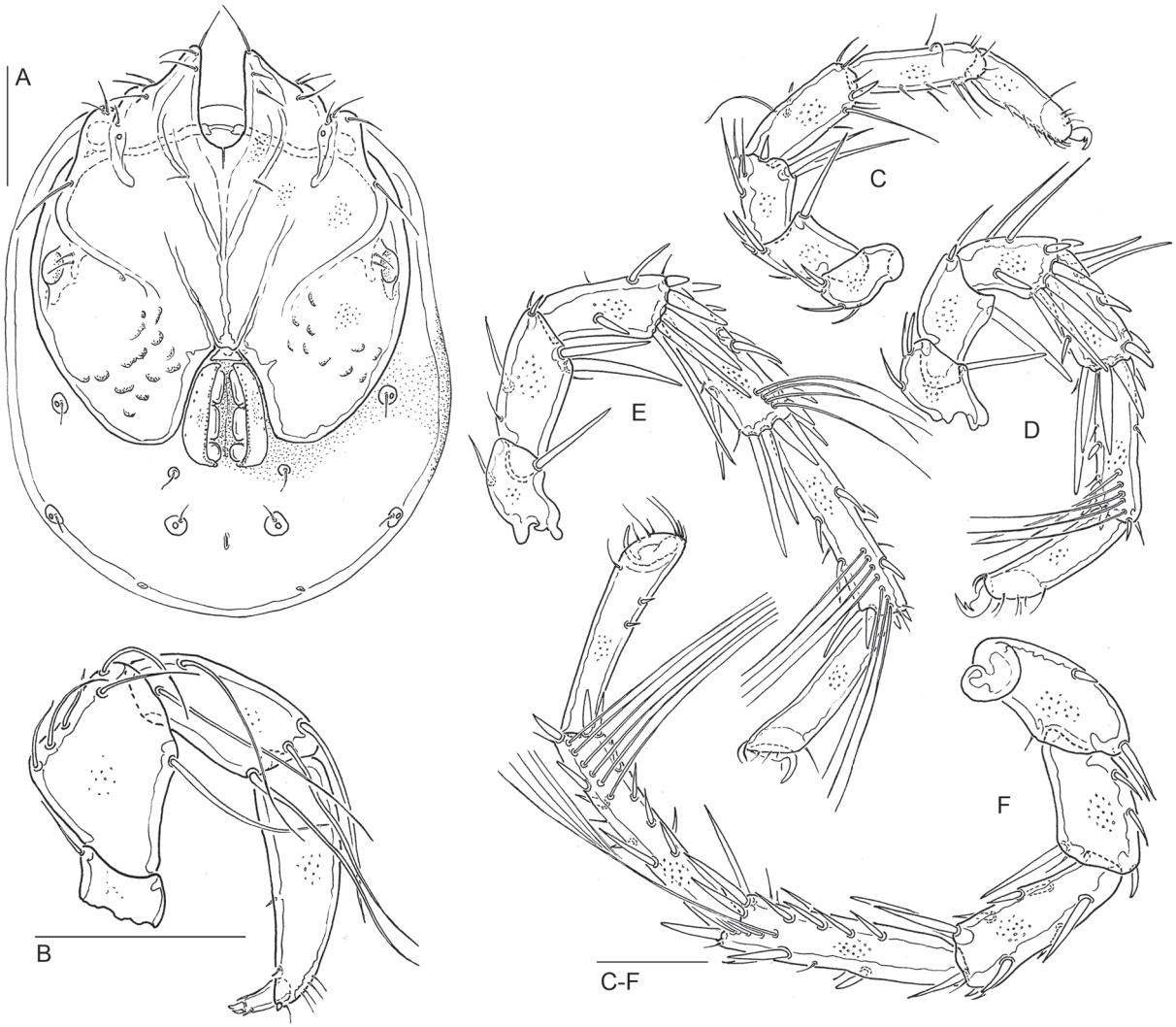

Fig. 9. *Lebertia* (*Pilolebertia*) *gibbosa* Lundblad, 1926, holotype, ♂ (NHRS). **A**. Venter. **B**. Palp. **C**. I-L. **D**. II-L. **E**. III-L. **F**. IV-L. Scale bars = 100 μm.

Palp measurements (L/H, ratio, % total L): P-1 31–33/43–45, 0.7, 8; P-2 100–103/63–65, 1.6, 24–25; P-3 110–113/48, 2.3–2.4, 27; P-4 130–138/38–39, 3.4–3.7, 32–33; P-5 33/5, 7.2, 8; proportions of segments (L ratio): P-2/P-3 0.91, P-2/P-4 0.73–0.79, P-3/P-4 0.80–0.87; distance ratio distal setae P-3 (A/B) 1.80; P-4 ventral sectors 57–67 %, 24–34 %, 8–9 %; palp total L 410–411.

Remarks

The meagre original description is without measurement data and refers in most details to character states typical for all species of the subgenus *Pilolebertia* (Lundblad 1926). The only diagnostic feature mentioned is the name-giving shape of P-2, elevated to form an obtuse-angled hump. Lundblad's fig. 5 shows a palp with P-3 having the mediodistal seta approaching the dorsodistal seta (calculated ratio A/B ca 2.0). P-3/-4 slender (L/H ratio 2.1, 2.9), P-3 proportionally long (L ratio P-3/4 0.85).

Lebertia gibbosa fits the characteristics of the *porosa*-like *Lebertia* species in the absence of a kink in the distoventral gnathosomal margin, but distinct differences are found in the characteristic, name-giving hump of P-2, the slender palp segments P-3 and P-4, the position of the ventral setae (both in distal half, proximal sector > 50%), and the small size of the distal peg seta on P-4. The P-4 size is similar to that in *L. inaequalis* (Koch, 1837), and application of the key in Gerecke (2009) is misleading, keying *L. gibbosa* to *L. inaequalis*. *Lebertia inaequalis* agrees with *L. gibbosa* also in the swimming setation, but differs, in addition to the ventral kink of the gnathosoma, in having a P-2 with its dorsal margin equally curved, not protruding to form a hump, and P-3 with mediodistal seta not, or only slightly, approaching the dorsodistal seta. A comparison with measurements of Norwegian specimens morphologically attributed to *L. inaequalis* reveals a wide overlap in many dimensions and proportions. The latter differ from *L. gibbosa* in having a more slender I-L-6 (L/H > 3.7), longer IV-L claws (> 55) and a higher P-2/P-3 ratio (> 1.0). DNA barcode data in BOLD indicate that *L. inaequalis*, similar to what is shown here for *L. porosa* aggr., represents a species complex with several BINs under this name. Upon taxonomic revisions, we expect that the wide variability for leg proportions of *L. inaequalis* described by Gerecke (2009) will cover a range of several distinct species.

Before our study, this species was only known from its type locality on the island of Gotland (Sweden). Our data show a wide distribution in southern Norway, in the north reaching up to southern Trøndelag County (63° N). As this species has been widely overlooked, the full geographical distribution of *L. gibbosa* cannot be defined without additional research.

Lebertia* (*Pilolebertia*) *vigintimaculata Thor, 1900

Lebertia (*Pilolebertia*) *20maculata* Thor, 1900: 272, pl. 10 figs 1–2.

Nomen dubium, probably identical with *L. obscura* Thor, 1900.

Type series

Missing. Type locality: Norway, "Storvandetz (Hammerfest); Hannesvand (Senjen)"; no date, no information on number of specimens, at least one female.

Material examined

NORWAY • 1 ♀, 1 dn; "10-7-1897 Dam i Bergselv paa Hindö. Sig Thor *Lebertia 20-maculata* Sig Thor + NB nymfe"; slide mounted; NHMO • 4 ♂♂, 11 ♀♀; "6-7-97 Svartelv [??] Sollivand nær Bodö. Sig Thor *Lebertia 20maculata* Sig Thor"; of these, 2 ♂♂ and 2 ♀♀ slide mounted; NHMO • 1 ♀; "*Lebertia vigintimaculata*, ♀, Hamersdengen (?) Dr. Sig Thor ges. 3.7.1897"; slide mounted; MNHB 1762 (see Gerecke 2009) • 1 ♀; "K. Viets 45262; *Lebertia vigintimaculata* Thor / Cotype. Norwegen. Svartelv ved Bodö. 6.7.1897 S. Thor leg. 2000"; slide mounted; SMF.

Remarks

Characters considered as species-diagnostic in the original description concern exclusively body colouration (Thor 1900). It was described as dark brown "with a narrow, dark dorsal line" (in Thor 1900: fig. 1, a Y-shaped line is visible; such a line, representing the excretory organ, is typically whitish in species of *Lebertia*). Furthermore, Thor observed dorsally a pattern of ca 20 darker dots ("strongly resembling *L. oudemansi*, but the latter with 12 such dots only"). The description includes the following additional details: idiosoma L/W 1500/1300–1400; integument rather thick and punctate. Shape of coxal and genital fields "as in *L. insignis* and *L. porosa*"; palps and legs very strong (palps as thick as I-L); III- and IV-L-5/6 each with 6–12 long swimming setae "in a bundle". His two figures (Thor 1900: pl. 10 figs 1–2) show a dorsal view of a specimen of uncertain sex and the partial venter of a female. From his fig. 2, a mL ratio Cx-I/II of about 2.0 can be calculated.

The arrangement of the name-giving twenty dots in Thor's fig. 1 makes it clear that they represent glandular sacs which are present in all water mites in a stable number of 16 pairs. In specimens of *Lebertia* of minor size (and lower age), only 12 of these sacs may be visible in dorsal view (as stated by Thor for *L. oudemansi* Koenike, 1898; see above). With increasing age and larger size, sacs of lateral glandularia move to a position that they become better visible in dorsal view, resulting in an increased number of dorsally visible "dots". Thor himself discussed the significance of glandularia for the coloration and stated that he had doubts about this taxon (Thor 1926).

The information provided in the original description does not allow any attribution to one of the clades defined in our study. From a morphological analysis of specimens identified by Sig Thor (Material examined above; the indication "Cotype" for SMF 45262 is incorrect) we conclude that they agree with our redescription of *Lebertia obscura*.

This species was proposed as a junior synonym of *Lebertia porosa* by K. Viets (1956) without acknowledging that *L. porosa* and *L. porosa obscura* would be junior synonyms of *Lebertia vigintimaculata*, since the latter species was described by Thor 1900 on page 272, while *L. porosa* and *porosa obscura* were described on page 273 (page priority). Due to the lack of type material, no taxonomic stability can be attained for *L. vigintimaculata,* and we regard it as a nomen dubium. Records of *L. vigintimaculata* from outside Norway are of questionable identity.

Lebertia* (*Pilolebertia*) *porosa britannica Thor, 1906

Lebertia (*Pilolebertia*) *porosa britannica* Thor, 1906: 776.

Nomen dubium.

Type series

Missing. Type locality: "England, Schottland" "… besonders unter den englischen Exemplaren einzelne Individuen …"; no date, no information on number of specimens. No material available.

Remarks

Having introduced *L. porosa britannica* as "nov. var.", it is unclear whether Thor intended to assign the taxon (sub)species value. In his description, Thor (1906) gave the name to specimens having a character combination not found in the material studied here, stating that Ac-3 was "nearly as long as Ac-1 and -2". In other taxa of the subgenus, Ac-3 is distinctly shorter. However, as Thor did not describe any further morphological details, and in view of the absence of locality information and type material, *L. porosa britannica* cannot be considered a junior synonym of *L. porosa* (as proposed in Viets 1956), but is to be treated as a nomen dubium.

Lebertia* (*Pilolebertia*) *porosa dorsalis Thor, 1906

Lebertia (*Pilolebertia*) *porosa dorsalis* Thor, 1906: 779.

Nomen dubium.

Type series

Missing. Type locality: Norway, "Bach bei Sarpsborg" (Østfold); no date, no information on number of specimens. No material available.

Remarks

Thor (1906) introduced this name for specimens having the mediodistal seta on P-3 closer to the dorsodistal one, without giving any further morphological details or discussion. Designating the taxon as "nov. var.", Thor left the question open whether he considered it a separate (sub)species. In the redescriptions of *L. porosa* and *L. obscura*, the position of this seta is subject to considerable individual variability, while a rather extreme case of dorsal shifting of the mediodistal seta P-3 is found in specimens belonging to *L. gibbosa* (P-3 A/B > 1.6). In the absence of further morphological information and due to the lacking type material, there is no reliable reason for reanimating *L. porosa dorsalis*. It cannot be interpreted as a junior synonym of *L. porosa* (as proposed in Viets 1956), and it has to be considered a nomen dubium.

Lebertia* (*Pilolebertia*) *porosa italica Thor, 1906

Lebertia (*Pilolebertia*) *porosa italica* Thor, 1906: 779.

Nomen dubium.

Type series

Missing. Type locality: Italy, Lago Maggiore, coll. Thor; no date, no information on number of specimens. No material available.

Remarks

Thor (1906) gave this name to specimens having a coxal field and appendages with an intense green-blue coloration. This is exactly the same colouration as was the basis for defining *L. obscura* and it remains unclear why Thor published this name. In the absence of type material, *L. porosa italica* cannot be considered a junior synonym of *L. porosa* (as proposed in Viets 1956), and it has to be considered a nomen dubium.

Lebertia* (*Pilolebertia*) *porosa distans Thor, 1926

Lebertia (*Pilolebertia*) *porosa distans* Thor, 1926: 145.

Nomen dubium.

Type series

Lost. Type locality: Russia, Kamtschatka, Ustj-Kamtschatsk, large island, 2 Jun. 1908, 1 specimen (Glas 21) (based on Thor 1926: pl. 11 fig. 3, obviously a female). No material available.

Remarks

In the original description, Thor (1926) recognized a similarity to *L. porosa* (without stating which characters) and to *L. vigintimaculata* (in colour pattern). From the description and an analysis of the figures given there (Thor 1926: pl. 11 figs 1–3: palp, misshaped III-L, and genital field), the following additional details are noted: large in size (idiosoma L/H 1500/1200); gnathosomal and genital bays very large; Ac at their tips rounded (instead of subrectangular); ventral seta P-2 not far from distal end, medial setae at distal end of P-3 equidistant; P-4 little curved, distally narrowed, ventral setae far away from each other, sectors 26, 48, and 26%. No data on legs (except for the description and depiction of a malformation of III-L in the single available specimen).

The description of this species, based on a single, malformed specimen, does not include information sufficient to define diagnostic characters; an interesting feature is the large centroventral sector of P-4, not found in any specimen of the *Lebertia porosa* aggr. treated here. *Lebertia porosa distans* cannot be interpreted as a junior synonym of *L. porosa* (as proposed in Viets 1956), and it must be considered a nomen dubium.

Other species examined

Lebertia insignis Neuman, 1880

Lebertia insignis Neuman, 1880: 69.

Material examined

NORWAY • 3 ♂♂; Agder, Songdalen, Stavbekken, ved Dynamitten; 58.15848° N, 7.81138° E, 45 m a.s.l.; 30 Aug. 2019; Gaute Kjærstad leg.; BOLD specimen ID HYDCA292 (slide mounted), HYDCA293 (slide mounted), HYDCA453; NTNU-VM 227933, 227934, 227942 • 3 ♂♂, 2 ♀♀; same collection data as for preceding; NTNU-VM 227935 (slide mounted), 227936 • 1 ♂; Telemark, Drangedal, Engåa (pool); 59.03855° N, 9.28759° E; 71 m a.s.l.; 19 Aug. 2019; Gaute Kjærstad leg.; BOLD specimen ID HYDCA334; NTNU-VM 227930 • 1 ♂, 1 ♀; same locality as for preceding; 17 Jun. 2020; BOLD specimen ID HYDCA365, HYDCA 366; NTNU-VM 227931, 227932 • 1 ♂; Agder, Søgne, Søgneelva, upstream bridge close to old Søgne Church; 58.08952° N, 7.83998° E; 2 m a.s.l.; 21 Jun. 2020; Gaute Kjærstad and Reinhard Gerecke leg.; BOLD specimen ID HYDCA434 (slide mounted); NTNU-VM 227937 • 1 ♂, 2 ♀♀, 1 dn; same collection data as for preceding; NTNU-VM 227940 • 1 ♂; Agder, Marnardal, Lågåna, Øvre Laudal; 58.26750° N, 7.45603° E; 175 m a.s.l.; 31 Aug. 2019; Gaute Kjærstad leg.; BOLD specimen ID HYDCA559; NTNU-VM 227939 • 1 ♂, 4 ♀♀; same collection data as for preceding; NTNU-VM 227938 • 1 ♂; Trøndelag, Stjørdal, Hegra, opposite of gas station at E14; 63.4631° N, 11.0853° E; 71 m a.s.l.; 3 Jul. 2020; Torbjørn Ekrem and Valentina Tyukosová leg.; BOLD specimen ID HYDCA457; NTNU-VM 227941.

Lebertia porosa aggr. sp. A

Material examined

GERMANY • 1 ♀; Baden-Württemberg, Tübingen, Lustnau, Ammer bei Aeule-Brücke; 48.526809° N, 9.079.652 E; 310 m a.s.l.; 29 Sep. 2020; Reinhard gerecke leg.; BOLD specimen ID HYDCA477; NTNU-VM 227801.

NORWAY • 1 ♂; Agder, Flekkefjord, Skålansåna, upstream from bridge; 58.3652° N, 6.85985° E; 179 m a.s.l.; 25 Aug. 2019; Gaute Kjærstad and Reinhard Gerecke leg.; BOLD specimen ID HYDCA258; NTNU-VM 227804 • 4 ♂♂, 3 ♀♀; Agder, Kristiansand, creek close to Nedre Timenes vei nr. 51, at

bridge; 58.16324° N, 8.10116° E; 1 m a.s.l.; 27 Aug. 2019; Gaute Kjærstad and Reinhard Gerecke leg.; BOLD specimen ID HYDCA269, HYDCA428, HYDCA250, HYDCA251, HYDCA427, HYDCA448, HYDCA449; NTNU-VM 227805 to 227809 (slide mounted), 227810, 227811 • 1 ♀; same collection data as for preceding; NTNU-VM 227825• 1 ♂; Agder, Kristiansand, Nedre Jegersbergvann, inlet flow stream; 58.16920° N, 08.00007° E; 21 m a.s.l.; 2 Sep. 2019; Reinhard Gerecke and Torbjørn Ekrem leg.; BOLD specimen ID HYDCA561; NTNU-VM 227812 • 1 ♂, 1 ♀; Agder, Froland, Bøylefoss, ved Bøylefoss kraftverk; 58.597° N, 8.718° E; 59 m a.s.l.; 19 Jun. 2020; Gaute Kjærstad leg.; BOLD specimen ID HYDCA562, HYDCA563; NTNU-VM 227813, 227814 • 1 ♂, 1 ♀; Møre og Romsdal, Eide, Nåsvassdraget, Sagelva, station 1; 62.89968° N, 7.42313° E; 8 m a.s.l.; 14 Sep. 2016; Gaute Kjærstad leg.; NTNU-VM 227820, 227821 • 1 ♂; Nordland, Vefsn, Drevjaelva, station 2; 66.033° N, 13.317° E; 38 m a.s.l.; 11 Aug. 2014; Gaute Kjærstad leg.; BOLD specimen ID HYDCA30 (slide mounted); NTNU-VM 227800 • 1 ♂; Nordland, Vefsn, Drevjaelva, station 1; 66.01103° N, 13.27527° E; 25 m a.s.l.; 8 Aug. 2016; Gaute Kjærstad leg.; BOLD specimen ID HYDCA544; NTNU-VM 227819 • 1 ♂, 1 ♀; Telemark, Nissedal, outlet Nisser, at power station; 59.00743° N, 8.55343° E; 240 m a.s.l.; 21 Aug. 2019; Gaute Kjærstad leg.; BOLD specimen ID HYDCA440, HYDCA441; NTNU-VM 227802, 227803 • 1 ♂, 2 ♀♀; same collection data as for preceding; slide mounted; NTNU-VM 227822 to 227824 • 1 ♂; Trøndelag, Stjørdal, Stjørdalselva at Hegra; 63.46305° N, 11.08623° E; 71 m a.s.l.; 3 Jul. 2020; Valentina Tyukosová and Torbjørn Ekrem leg.; BOLD specimen ID HYDCA573; NTNU-VM 227818 • 1 ♂, 2 ♀♀; Trøndelag, Stjørdal, Hegrasbekken; 63.46608° N, 11.10321° E; 11 m a.s.l.; 3 Jul. 2020; Valentina Tyukosová and Torbjørn Ekrem leg.; BOLD specimen ID HYDCA413, HYDCA414, HYDCA415; NTNU-VM 227815 to 227817 • 1 ♀; same locality as for preceding; NTNU-VM 227826.

Lebertia porosa aggr. sp. B

Material examined

NORWAY • 1 ♀; Nordland, Vefsn, Fustvatnet, station 1; 65.907° N, 13.361° E; 38 m a.s.l.; 13 Aug. 2014; Gaute Kjærstad leg.; BOLD specimen ID HYDCA5 (slide mounted); NTNU-VM 227827 • 1 ♀; Trøndelag, Midtre Gauldal, Holtsjøen, station 2; 63.07638° N, 10.82113° E; 543 m a.s.l.; 26 Jun. 2017; Gaute Kjærstad leg.; BOLD specimen ID HYDCA227 (slide mounted); NTNU-VM 227828 • 1 ♀; Trøndelag, Orkdal, Ålvatnet, station 1; 63.30147° N, 9.79980° E; 216 m a.s.l.; 26 Jun. 2018; Gaute Kjærstad leg.; BOLD specimen ID HYDCA551; NTNU-VM 227829.

Lebertia porosa aggr. sp. D

Material examined

NORWAY • 2 adults, 1 ♀; Nordland, Vefsn, Drevvatnet, station 1; 66.052° N, 13.364° E; 47 m a.s.l.; 11 Aug. 2014; Gaute Kjærstad leg.; BOLD specimen ID HYDCA19, HYDCA75, HYDCA77 (all slide mounted); NTNU-VM 227831 to 227833 • 1 dn; Nordland, Vefsn, Drevvatnet, station 3; 66.048° N, 13.387° E; 47 m a.s.l.; 10 Jun. 2013; Gaute Kjærstad leg.; BOLD specimen ID HYDCA56 (slide mounted); NTNU-VM 227830 • 1 ♀; Nordland, Vefsn, Fustvatnet, station 1; 65.907° N, 13.361° E; 38 m a.s.l.; 13 Aug. 2014; Gaute Kjærstad leg.; BOLD specimen ID HYDCA10 (slide mounted); NTNU-VM 227834 • 1 ♀; Trøndelag, Stjørdal, Stjørdalsvassdraget, Stjørdalelva, station 1; 63.46251° N, 11.09256° E; 33 m a.s.l.; 26 Apr. 2016; Gaute Kjærstad leg.; BOLD specimen ID HYDCA157 (slide mounted); NTNU-VM 227835 • 1 ♂, 1 ♀; Trøndelag, Midtre Gauldal, Holtsjøen, station 3; 63.09435° N, 10.78832° E; 543 m a.s.l.; 26 Jun. 2017; Gaute Kjærstad leg.; BOLD specimen ID HYDCA546, HYDCA547; NTNU-VM 227836, 227837 • 1 ♂, 4 dn; same collection data as for preceding; NTNU-VM 227838.

Lebertia porosa aggr. sp. E

Material examined

NORWAY • 1 ♂; Møre og Romsdal, Eide, Nåselva, station 1; 62.89278° N, 7.37926° E; 45 m a.s.l.; 14 Sep. 2016; Gaute Kjærstad leg.; BOLD specimen ID HYDCA552; NTNU-VM 227843 • 1 ♂; Nordland, Vefsn, Fustvatnet, station 3; 65.906° N, 13.432° E; 38 m a.s.l.; 13 Aug. 2014; Gaute Kjærstad leg.; BOLD specimen ID HYDCA80 (slide mounted); NTNU-VM 227839 • 1 ♀; Troms, Storfjord, Skibotnelva, station 5; 69.29167° N, 20.42249° E; 64 m a.s.l.; 24 Aug. 2016; Gaute Kjærstad leg.; BOLD specimen ID HYDCA553; NTNU-VM 227844 • 1 ♀; same collection data as for preceding; NTNU-VM 227845 • 1 ♀; Troms, Storfjord, Skibotnelva, station 2; 69.17014° N, 20.74697° E; 450 m a.s.l.; 12 Sep. 2016; Gaute Kjærstad leg.; BOLD specimen ID HYDCA554; NTNU-VM 227846 • 1 ♀; Trøndelag, Meråker, Stjørdalselva, station 6; 63.44283° N, 11.62808° E; 92 m a.s.l.; 26 Apr. 2016; Gaute Kjærstad leg.; BOLD specimen ID HYDCA162 (slide mounted); NTNU-VM 227841 • 1 dn; Trøndelag, Stjørdal, Stjørdalselva, station 31; 63.42832° N, 11.71137° E; 75 m a.s.l.; 30 Aug. 2018; Gaute Kjærstad leg.; BOLD specimen ID HYDCA541; NTNU-VM 227842 • 1 ♂; same collection data as for preceding; NTNU-VM 227847 • 1 ♂; Trøndelag, Trondheim, Bymarka, Tungabekken, station 1; 63.41826° N, 10.31228° E; 205 m a.s.l.; 21 Sep. 2016; Gaute Kjærstad leg.; BOLD specimen ID HYDCA155 (slide mounted); NTNU-VM 227840.

***Lebertia* (*Lebertia*)** sp. (outgroup)

Material examined

RUSSIA • 1 ♂; Sibiria, Irkutsk Oblast, Baikal, stream 1 (Reka Kuchelga); 53.01665° N, 106.74055° E; 460 m a.s.l.; 20 Sep. 2018; Gaute Kjærstad and Torbjørn Ekrem leg.; BOLD specimen ID HYDCA351; NTNU-VM 228687.

Discussion

Species delimitation

The results from the species delimitation analyses support the existence of seven potential species-level clades within the *Lebertia porosa* species aggregate from Norway. Multiple lines of evidence using both molecular and morphological data show that while previously named taxa can be assigned to some clades, others likely constitute species new to science. These findings are in agreement with observations from other species complexes within Hydrachnidia that have resulted in the description of new species of water mites (Pešić & Smit 2016; Pešić *et al.* 2017; Blattner *et al.* 2019; Montes-Ortiz & Elías-Gutiérrez 2020) and provide further proof that Hydrachnidia hides a great amount of undescribed diversity (Di Sabatino *et al.* 2008).

The single marker models do not always show the expected number of OTUs, but the differences occur in a manner consistent with the method's reported error patterns and with the observed genetic variation in individual markers. For instance, none of the methods could separate *Lebertia porosa* aggr. sp. A from B using 18S data due to the limited genetic variation in this marker. GMYC obviously overestimates the number of OTUs in markers with many variable sites (Table 2), while it comes within a reasonable range for the 18S marker. 18S shows by far the lowest genetic variation among the markers, perhaps within a range that GMYC can cope with (Esselstyn *et al.* 2012; Talavera *et al.* 2013; Dellicour & Flot 2015). The COI marker shows considerably higher genetic divergence rates between groups than within groups, and ABGD, ASAP, and PTP groups the sequences in our dataset according to the expected number of OTUs for this marker (Puillandre *et al.* 2021). In general, the methods perform less poorly using nuclear markers, where the genetic distances are shorter overall, and no large difference between

the intraspecific and interspecific distances is apparent. The numbers of OTUs are close to or equal, the expected value (Table 2), but for 18S and 28S this is a result of these models both overestimating and underestimating the number of OTUs at the same time due to the large intraspecific divergence in *Lebertia obscura* and the small interspecific divergence between *Lebertia porosa* aggr. sp. D and E (Puillandre *et al.* 2012, 2021). While studies using larger datasets, such as Pentinsaari *et al.* (2017), might be forced to rely on methods designed for single markers only and use further statistical analysis to resolve the discrepancies between the different results from each model, the small number of individuals analysed in our study allows for the use of multi-locus methods. BPP uses all markers and thus reduces the influence of possible incomplete lineage sorting in individual marker genealogies (Jacobs *et al.* 2018; Yang & Rannala 2010). BPP always delimits all seven clades in our *L. porosa* dataset regardless of priors used, but the posterior probability decreases with higher θ values. Since θ represents the average genetic difference between members of the same population, runs using higher values tend to result in a more conservative assessment of the number of OTUs (McKay *et al.* 2013; Flouri *et al.* 2018).

Although speculations about the presence of *Wolbachia* in water mites exist (Stryjecki *et al.* 2015), infections have previously only been documented as untargeted contaminants (Blattner *et al.* 2019; Blattner pers comm. May 2022), and a confirmed presence is lacking in the literature and genetic databases. Thus, the identified *Wolbachia* sequences obtained from specimens of *Lebertia obscura* and *Lebertia porosa* are the first confirmed positive finds within this organism group. PCRs using primers designed to amplify the *Wolbachia* 16S marker were also positive for specimens in other clades, but since their identity currently cannot be confirmed through Sanger sequence comparisons due to co-amplification of more than one DNA segment (inconclusive chromatograms), we do not consider them proof of *Wolbachia* infections. However, the presence of *Wolbachia* within the other clades remains a possibility. 16S rDNA has an estimated divergence rate of 1–2% per 50 million years in bacteria and shorter fragments of the ~1500 bp gene are not useful in identifying newly diverged strains and species (Werren *et al.* 1995; Johnson *et al.* 2019). Our attempts to amplify more divergent sequences of the *Wolbachia* genome, such as wsp and ftsZ, were unfortunately unsuccessful. The infected hosts are widely distributed across Norway, come from various habitats, and consist of four females and two males. In species where *Wolbachia* infections lead to cytoplasmic incompatibility, the COI marker tends to give a very different number of OTUs in molecular delimitation compared to nuclear markers (Jiang *et al.* 2018; Sucháčková Bartoňová *et al.* 2021). Cytoplasmic incompatibility, therefore, does not seem to be a likely explanation for the observed divergence in our COI dataset. We also speculate whether the *Wolbachia* DNA might not have originated from a water mite infection, but rather from an internal parasite such as a nematode. Our specimens were not checked for the presence of parasites during this study and the closest matches of our *Wolbachia* sequences do not allow us to discard this possibility.

Taxonomy

The Norwegian arachnologist Sig Thor (1856–1936) is famous for the publication of numerous taxa, but sadly also for organizing the destruction of his slide collection, causing the loss of a large portion of his type material (Lundblad 1938; Viets 1939). As molecular taxonomy progresses rapidly, the reinvestigation and revised definition of important species erected by Thor is an important task. This way, taxonomic stability is provided for many species that currently are questioned, not only in Fennoscandia, but all over Europe and on other continents. By revisiting the type locality of *Lebertia porosa* Thor, 1900, a species for which the types are lost and that was highly discussed in the past century (Gerecke 2009), we were able to sample specimens attributable to this species. To our slight surprise, specimens from this stream that morphologically fit Gerecke's (2009) definition of *Lebertia porosa* belonged to three clearly separable genetic lineages. However, detailed comparisons with original descriptions and the type of *L. obscura* enabled us to identify which of these lineages belonged to *L. porosa* and prepare a revised morphological definition of that species (above).

The new data presented here is a good example of the advantage of integrative taxonomy. Even without more statistically advanced morphometric analyses to identify geometric characters of taxonomic importance (e.g., Xinyao *et al.* 2022), morphological characters useful to separate closely related species of *Lebertia* could be found (e.g., Table 3). Moreover, revisiting a number of morphological traits made it clear that a re-evaluation of several characters used for species definitions within *Lebertia* should be considered:

(1) Thor (1900) considered the name-giving porous structuration of the upper epidermal layer as a character state of importance for distinguishing *Lebertia porosa* from *L. inaequalis* and *L. insignis*. In the following years, several authors followed his example and described further species based on this feature, focusing on minor differences in the integument structure as diagnostic differences. To fully understand the taxonomic significance of skin structures in lebertiid mites, it would be necessary to investigate adult specimens of a wide age spectrum and include scanning electron microscope (SEM) techniques. However, as the porosity of the upper integument layers in water mites is of importance for respiration (Popp 1991), an age-dependent change of density and arrangement of these pores is to be expected.

(2) Many early authors gave particular weight to the description of the idiosoma colour patterns and the coloration of appendages. In later decades, such characters went out of style, mostly for practical reasons: more and more species were described based on material fixed in different preservatives that was more or less discoloured. Furthermore, it became clear that colouration in mites may change with increasing age, or from site to site, possibly depending on water chemistry. In the present study we had to widely exclude these characters because we were dealing nearly exclusively with discoloured material from museum collections. However, there is surely no justification for completely disregarding colouration in a taxonomic group as strongly characterized by a wide variety of colour patterns as water mites. In the future, the colours of living specimens merit careful attention in species descriptions.

(3) Morphological characters previously neglected in the taxonomy of *Lebertia*, but obviously of high importance for species discrimination, are found in the proportions of the first and the fourth legs and their claws. In future studies, the second and third leg segments should also be taken into consideration when searching for diagnostic character states. Concerning swimming setae, both the numbers and their exact arrangement should be taken into consideration.

Acknowledgements

We would like to thank Gaute Kjærstad, Aina Mærk Aspaas and Karstein Hårsaker at NTNU-VM for their help in the field and laboratory, and the County Governor of Agder for collecting permits in protected areas. We also thank the Norwegian Biodiversity Information Centre (NBIC) for support through Norwegian Taxonomy Initiative grant no KNR 13-18 for the project 'Water Mites and Midges in Southern Norway' to the NTNU University Museum. DNA barcode data were in part generated in collaboration with the Norwegian Barcode of Life Initiative (NorBOL) with funding from NBIC though the Norwegian Taxonomy Initiative. Andrej Shatrov (St. Petersburg) helped us with valuable information about, and photographs of, material classified as *Lebertia riabuschinskii* at ZISP.

References

Anderson A.M., Stur E. & Ekrem T. 2013. Molecular and morphological methods reveal cryptic diversity and three new species of Nearctic *Micropsectra* (Diptera: Chironomidae). *Freshwater Science* 32: 892–921. https://doi.org/10.1899/12-026.1

Besseling A.J. 1958. Notes sur des hydrachnelles provenant du Grand-Fuché de Luxembourg. *Institut Grand-Ducal de Luxembourg, Archives des Sciences naturelles, physiques et mathématiques (New Series)* 25: 219–226.

Blattner L., Gerecke R. & von Fumetti S. 2019. Hidden biodiversity revealed by integrated morphology and genetic species delimitation of spring dwelling water mite species (Acari, Parasitengona: Hydrachnidia). *Parasites & Vectors* 12: e492. https://doi.org/10.1186/s13071-019-3750-y

Breeuwer J.A.J. & Jacobs G. 1996. *Wolbachia*: intracellular manipulators of mite reproduction. *Experimental & Applied Acarology* 20: 421–434. https://doi.org/10.1007/BF00053306

Brown A.N. & Lloyd V.K. 2015. Evidence for horizontal transfer of *Wolbachia* by a *Drosophila* mite. *Experimental and Applied Acarology* 66: 301–311. https://doi.org/10.1007/s10493-015-9918-z

Camacho C., Coulouris G., Avagyan V., Ma N., Papadopoulos J., Bealer K. & Madden T.L. 2009. BLAST+: architecture and applications. *BMC Bioinformatics* 10: e421. https://doi.org/10.1186/1471-2105-10-421

Camargo A., Morando M., Avila L.J. & Sites J.W. Jr. 2012. Species delimitation with ABC and other coalescent-based methods: a test of accuracy with simulations and an empirical example with lizards of the *Liolaemus darwinii* complex (Squamata: Liolaemidae). *Evolution* 66: 2834–2849. https://doi.org/10.1111/j.1558-5646.2012.01640.x

Carstens B.C., Pelletier T.A., Reid N.M. & Satler J.D. 2013. How to fail at species delimitation. *Molecular Ecology* 22: 4369–4383. https://doi.org/10.1111/mec.12413

Clement M., Posada D. & Crandall K.A. 2000. TCS: a computer program to estimate gene genealogies. *Molecular Ecology* 9: 1657–1659. https://doi.org/10.1046/j.1365-294x.2000.01020.x

Cook D.R. 1974. Water mite genera and subgenera. *Memoirs of the American Entomological Institute* 21: 1–860.

Cordaux R., Michel-Salzat A. & Bouchon D. 2001. *Wolbachia* infection in crustaceans: novel hosts and potential routes for horizontal transmission. *Journal of Evolutionary Biology* 14: 237–243. https://doi.org/10.1046/j.1420-9101.2001.00279.x

Dabert M., Witalinski W., Kazmierski A., Olszanowski Z. & Dabert J. 2010. Molecular phylogeny of acariform mites (Acari, Arachnida): strong conflict between phylogenetic signal and long-branch attraction artifacts. *Molecular Phylogenetics and Evolution* 56: 222–241. https://doi.org/10.1016/j.ympev.2009.12.020

Dabert M., Proctor H. & Dabert J. 2016. Higher-level molecular phylogeny of the water mites (Acariformes: Prostigmata: Parasitengonina: Hydrachnidiae). *Molecular Phylogenetics and Evolution* 101: 75–90. https://doi.org/10.1016/j.ympev.2016.05.004

Dellicour S. & Flot J.-F. 2015. Delimiting species-poor data sets using single molecular markers: a study of barcode gaps, haplowebs and GMYC. *Systematic Biology* 64: 900–908. https://doi.org/10.1093/sysbio/syu130

Dellicour S. & Flot J.-F. 2018. The hitchhiker's guide to single-locus species delimitation. *Molecular Ecology Resources* 18: 1234–1246. https://doi.org/10.1111/1755-0998.12908

Di Sabatino A., Smit H., Gerecke R., Goldschmidt T., Matsumoto N. & Cicolani B. 2008. Global diversity of water mites (Acari, Hydrachnidia; Arachnida) in freshwater. *Hydrobiologia* 595: 303–315. https://doi.org/10.1007/s10750-007-9025-1

Duarte M.E., de Mendonça R.S., Skoracka A., Silva E.S. & Navia D. 2019. Integrative taxonomy of *Abacarus* mites (Eriophyidae) associated with hybrid sugarcane plants, including description of a new species. *Experimental and Applied Acarology* 78: 373–401. https://doi.org/10.1007/s10493-019-00388-y

Edgar R.C. 2004. MUSCLE: multiple sequence alignment with high accuracy and high throughput. *Nucleic Acids Research* 32 (5): 1792–1797. https://doi.org/10.1093/nar/gkh340

Edler D., Klein J., Antonelli A. & Silvestro D. 2021. raxmlGUI 2.0: a graphical interface and toolkit for phylogenetic analyses using RAxML. *Methods in Ecology and Evolution* 12: 373–377. https://doi.org/10.1111/2041-210X.13512

Esselstyn J.A., Evans B.J., Sedlock J.L., Anwarali Khan F.A. & Heaney L.R. 2012. Single-locus species delimitation: a test of the mixed Yule–coalescent model, with an empirical application to Philippine round-leaf bats. *Proceedings of the Royal Society B: Biological Sciences* 279: 3678–3686. https://doi.org/10.1098/rspb.2012.0705

Ezard T., Fujisawa T. & Barraclough T.G. 2009. Splits: species' limits by threshold statistics, 1.0-20. R package version. Available from http://R-Forge.R-project.org/projects/splits/ [accessed 19 Jul. 2022].

Ferrer-Suay M., Staverløkk A., Selfa J., Pujade-Villar J., Naik S. & Ekrem T. 2018. Nuclear and mitochondrial markers suggest new species boundaries in *Alloxysta* (Hymenoptera: Cynipoidea: Figitidae). *Arthropod Systematics & Phylogeny* 76: 463–473.

Flouri T., Jiao X., Rannala B. & Yang Z. 2018. Species tree inference with BPP using genomic sequences and the multispecies coalescent. *Molecular Biology and Evolution* 35: 2585–2593. https://doi.org/10.1093/molbev/msy147

Gerecke R. 2003. Water mites of the genus *Atractides* Koch, 1837 (Acari: Parasitengona: Hygrobatidae) in the western Palaearctic region: a revision. *Zoological Journal of the Linnean Society* 138: 141–378. https://doi.org/10.1046/j.1096-3642.06-0.00051.x

Gerecke R. 2009. Revisional studies on the European species of the water mite genus *Lebertia* Neuman, 1880 (Acari: Hydrachnidia: Lebertiidae). *Abhandlungen der Senckenberg Gesellschaft für Naturforschung* 566: 1–144.

Guindon S., Dufayard J.-F., Lefort V., Anisimova M., Hordijk W. & Gascuel O. 2010. New algorithms and methods to estimate maximum-likelihood phylogenies: assessing the performance of PhyML 3.0. *Systematic Biology* 59: 307–321. https://doi.org/10.1093/sysbio/syq010

Hall B.G. 2013. Building phylogenetic trees from molecular data with MEGA. *Molecular Biology and Evolution* 30: 1229–1235. https://doi.org/10.1093/molbev/mst012

Hebert P.D.N., Ratnasingham S. & deWaard J.R. 2003. Barcoding animal life: cytochrome c oxidase subunit 1 divergences among closely related species. *Proceedings of the Royal Society B: Biological Sciences* 270 (Suppl. 1): S96–S99. https://doi.org/10.1098/rsbl.2003.0025

Hebert P.D.N., Ratnasingham S., Zakharov E.V., Telfer A.C., Levesque-Beaudin V., Milton M.A., Pedersen S., Jannetta P. & deWaard J.R. 2016. Counting animal species with DNA barcodes: Canadian insects. *Philosophical Transactions of the Royal Society B: Biological Sciences* 371 (1702): e20150333. https://doi.org/10.1098/rstb.2015.0333

Jacobs S.J., Kristofferson C., Uribe-Convers S., Latvis M. & Tank D.C. 2018. Incongruence in molecular species delimitation schemes: what to do when adding more data is difficult. *Molecular Ecology* 27: 2397–2413. https://doi.org/10.1111/mec.14590

Jiang W., Zhu J., Wu Y., Li L., Li Y., Ge C., Wang Y., Endersby N.M., Hoffmann A.A. & Yu W. 2018. Influence of *Wolbachia* infection on mitochondrial DNA variation in the genus *Polytremis* (Lepidoptera: Hesperiidae). *Molecular Phylogenetics and Evolution* 129: 158–170. https://doi.org/10.1016/j.ympev.2018.08.001

Johnson J.S., Spakowicz D.J., Hong B.-Y., Petersen L.M., Demkowicz P., Chen L., Leopold S.R., Hanson B.M., Agresta H.O., Gerstein M., Sodergren E. & Weinstock G.M. 2019. Evaluation of 16S

rRNA gene sequencing for species and strain-level microbiome analysis. *Nature Communications* 10: e5029. https://doi.org/10.1038/s41467-019-13036-1

Kozlov A.M., Darriba D., Flouri T., Morel B. & Stamatakis A. 2019. RAxML-NG: a fast, scalable and user-friendly tool for maximum likelihood phylogenetic inference. *Bioinformatics* 35: 4453–4455. https://doi.org/10.1093/bioinformatics/btz305

Kumar S., Stecher G., Li M., Knyaz C. & Tamura K. 2018. MEGA X: Molecular Evolutionary Genetics Analysis across computing platforms. *Molecular Biology and Evolution* 35: 1547–1549. https://doi.org/10.1093/molbev/msy096

Lanfear R., Calcott B., Ho S.Y.W. & Guindon S. 2012. PartitionFinder: combined selection of partitioning schemes and substitution models for phylogenetic analyses. *Molecular Biology and Evolution* 29: 1695–1701. https://doi.org/10.1093/molbev/mss020

Lanfear R., Frandsen P.B., Wright A.M., Senfeld T. & Calcott B. 2017. PartitionFinder 2: new methods for selecting partitioned models of evolution for molecular and morphological phylogenetic analyses. *Molecular Biology and Evolution* 34: 772–773. https://doi.org/10.1093/molbev/msw260

Leigh J.W. & Bryant D. 2015. popart: full-feature software for haplotype network construction. *Methods in Ecology and Evolution* 6: 1110–1116. https://doi.org/10.1111/2041-210X.12410

Lin X.-L., Stur E. & Ekrem T. 2018. DNA barcodes and morphology reveal unrecognized species in Chironomidae (Diptera). *Insect Systematics & Evolution* 49: 329–398. https://doi.org/10.1163/1876312X-00002172

Lundblad O. 1926. Neue Hydracarinen aus Schweden. V–VI. Vorläufige Mitteilung. *Entomologisk Tidskrift* 47: 205–208.

Lundblad O. 1938. Sig Thor. *Entomologisk Tidskrift* 59: 107–111.

Lundblad O. 1956. Zur Kenntnis süd- und mitteleuropäischer Hydrachnellen. *Arkiv för Zoologi* 10: 1–306.

Lundblad O. 1968. Die Hydracarinen Schwedens. III. *Arkiv för Zoologi* 21: 1–633.

Luo A., Ling C., Ho S.Y.W. & Zhu C.-D. 2018. Comparison of methods for molecular species delimitation across a range of speciation scenarios. *Systematic Biology* 67: 830–846. https://doi.org/10.1093/sysbio/syy011

McKay B.D., Mays H.L. Jr, Wu Y., LiH., Yao C.-T., Nishiumi I. & Zou F. 2013. An empirical comparison of character-based and coalescent-based approaches to species delimitation in a young avian complex. *Molecular Ecology* 22: 4943–4957. https://doi.org/10.1111/mec.12446

Montes-Ortiz L. & Elías-Gutiérrez M. 2020. Water mite diversity (Acariformes: Prostigmata: Parasitengonina: Hydrachnidiae) from karst ecosystems in southern of Mexico: a barcoding approach. *Diversity* 12 (9): e329. https://doi.org/10.3390/d12090329

Neuman C.J. 1880. Om Sveriges Hydrachnider. *Kungliga Svenska Vetenskaps-Akademiens Handlingar, Stockholm* (New Series) 17: 1–123.

Pentinsaari M., Vos R. & Mutanen M. 2017. Algorithmic single-locus species delimitation: effects of sampling effort, variation and nonmonophyly in four methods and 1870 species of beetles. *Molecular Ecology Resources* 17: 393–404. https://doi.org/10.1111/1755-0998.12557

Pešić V. & Smit H. 2016. Evidence of cryptic and pseudocryptic speciation in *Brachypodopsis baumi* species complex (Acari, Hydrachnidia, Aturidae) from Borneo, with description of three new species. *Systematic and Applied Acarology* 21: 1092–1106. https://doi.org/10.11158/saa.21.8.10

Pešić V., Asadi M., Cimpean M., Dabert M., Esen Y., Gerecke R., Martin P., Savic A., Smit H. & Stur E. 2017. Six species in one: evidence of cryptic speciation in the *Hygrobates fluviatilis* complex (Acariformes, Hydrachnidia, Hygrobatidae). *Systematic and Applied Acarology* 22: 1327–1377. https://doi.org/10.11158/saa.22.9.4

Pons J., Barraclough T.G., Gomez-Zurita J., Cardoso A., Duran D.P., Hazell S., Kamoun S., Sumlin W.D. & Vogler A.P. 2006. Sequence-based species delimitation for the DNA taxonomy of undescribed insects. *Systematic Biology* 55 (4): 595–609. https://doi.org/10.1080/10635150600852011

Popp E. 1991. Beobachtungen und Versuche zur Atmung von *Arrenurus* (*Megaluracarus*) *globator* (Müll.). 1. Morphologie (Acari, Hydrachnidia, Arrenuroidea). *Spixiana* 14: 249–257.

Puillandre N., Lambert A., Brouillet S. & Achaz G. 2012. ABGD, Automatic Barcode Gap Discovery for primary species delimitation. *Molecular Ecology* 21: 1864–1877. https://doi.org/10.1111/j.1365-294X.2011.05239.x

Puillandre N., Brouillet S. & Achaz G. 2021. ASAP: Assemble Species by Automatic Partitioning. *Molecular Ecology Resources* 21: 609–620. https://doi.org/10.1111/1755-0998.13281

Quast C., Pruesse E., Yilmaz P., Gerken J., Schweer T., Yarza P., Peplies J. & Glöckner F.O. 2013. The SILVA ribosomal RNA gene database project: improved data processing and web-based tools. *Nucleic Acids Research* 41 (D1): D590–D596. https://doi.org/10.1093/nar/gks1219

Ratnasingham S. & Hebert P.D.N. 2007. BOLD: the Barcode of Life Data System (boldsystems.org). *Molecular Ecology Notes* 7 (3): 355–364. https://doi.org/10.1111/j.1471-8286.2007.01678.x

R-Core-Team 2020. R: a language and environment for statistical computing. Available from https://www.Rproject.org/ [accessed 19 Jul. 2022].

Sazama E.J., Bosch M.J., Shouldis C.S., Ouellette S.P. & Wesner J.S. 2017. Incidence of *Wolbachia* in aquatic insects. *Ecology and Evolution* 7: 1165–1169. https://doi.org/10.1002/ece3.2742

Sela I., Ashkenazy H., Katoh K. & Pupko T. 2015. GUIDANCE2: accurate detection of unreliable alignment regions accounting for the uncertainty of multiple parameters. *Nucleic Acids Research* 43: W7–W14. https://doi.org/10.1093/nar/gkv318

Smith I.M. & Cook D.R. 1991. Water Mites. *In*: Thorp J. & Covich A. (eds) *Ecology and Classification of North American Freshwater Invertebrates*: 523–592. Academic Press, San Diego.

Stryjecki R., Czepiel-Mil K., Gryzinska M. & Zawal A. 2015. A very rare case of intersexuality in water mites of the genus *Arrenurus* Dugès, 1834 (Acari, Hydrachnidia). *Invertebrate Reproduction & Development* 59: 155–165. https://doi.org/10.1080/07924259.2015.1050560

Sucháčková Bartoňová A., Konvička M., Marešová J., Wiemers M., Ignatev N., Wahlberg N., Schmitt T. & Faltýnek Fric Z. 2021. *Wolbachia* affects mitochondrial population structure in two systems of closely related Palaearctic blue butterflies. *Scientific Reports* 11: e3019. https://doi.org/10.1038/s41598-021-82433-8

Talavera G., Dincă V. & Vila R. 2013. Factors affecting species delimitations with the GMYC model: insights from a butterfly survey. *Methods in Ecology and Evolution* 4: 1101–1110. https://doi.org/10.1111/2041-210X.12107

Thor S. 1900. Hydrachnologische Notizen I–III. *Nyt Magazin for Naturvidenskaberne* 38: 267–279. Available from https://www.biodiversitylibrary.org/page/35231603 [accessed 18 Jul. 2022].

Thor S. 1902. Untersuchungen über die Haut verschiedener dickhäutiger Acarina. *Arbeiten aus dem zoologischen Instituten der Universität Wien und der zoologischen Station in Triest* 14: 291–306.

Thor S. 1906. Lebertia-Studien VI–VIII. *Zoologischer Anzeiger* 29: 761–790. Available from https://www.biodiversitylibrary.org/page/10360125 [accessed 18 Jul. 2022].

Thor S. 1926. Die Acarina der Kamtschatka-Expedition 1908–1909. *Annuaire du Musée zoologique de l'Academie Impériale des Sciences d'U.R.S.S., Leningrad* 27: 131–174.

Viets K. 1936. Wassermilben oder Hydracarina (Hydrachnellae und Halacaridae). *In*: Dahl F. (ed.) *Tierwelt Deutschlands*: 1–288, 289–574. G. Fischer, Jena, Germany.

Viets K. 1939. Sig Thor. Ein Nachruf. *Internationale Vereinigung für theoretische und angewandte Limnologie: Verhandlungen* 9: 356–357. https://doi.org/10.1080/03680770.1940.11898683

Viets K. 1956. *Die Milben des Süßwassers und des Meeres: Hydrachnellae et Halacaridae (Acari). II. und III. Teil: Katalog und Nomenklator*. G. Fischer, Jena, Germany.

Werren J.H. & Windsor D.M. 2000. *Wolbachia* infection frequencies in insects: evidence of a global equilibrium? *Proceedings of the Royal Society B: Biological Sciences* 267 (1450): 1277–1285. https://doi.org/10.1098/rspb.2000.1139

Werren J.H., Zhang W. & Guo L.R. 1995. Evolution and phylogeny of *Wolbachia*: reproductive parasites of arthropods. *Proceedings of the Royal Society B: Biological Sciences* 261 (1360): 55–63. https://doi.org/10.1098/rspb.1995.0117

Werren J.H., Baldo L. & Clark M.E. 2008. *Wolbachia*: master manipulators of invertebrate biology. *Nature Reviews, Microbiology* 6: 741–751. https://doi.org/10.1038/nrmicro1969

Whitworth T.L., Dawson R.D., Magalon H. & Baudry E. 2007. DNA barcoding cannot reliably identify species of the blowfly genus *Protocalliphora* (Diptera: Calliphoridae). *Proceedings of the Royal Society B: Biological Sciences* 274: 1731–1739. https://doi.org/10.1098/rspb.2007.0062

Xinyao G., Yuling Z., Haitao L. & Jianjun G. 2022. A case of integrative taxonomy based on traditional morphology, molecular systematics and geometric morphometrics in the taxonomy of Torrenticolidae (Acari, Hydrachnidiae). *Systematic and Applied Acarology* 27: 905–921. https://doi.org/10.11158/saa.27.5.6

Yang Z. 2015. The BPP program for species tree estimation and species delimitation. *Current Zoology* 61: 854–865. https://doi.org/10.1093/czoolo/61.5.854

Yang Z. & Rannala B. 2010. Bayesian species delimitation using multilocus sequence data. *Proceedings of the National Academy of Sciences* 107 (20): 9264–9269. https://doi.org/10.1073/pnas.0913022107

Zhang C., Zhang D.-X., Zhu T. & Yang Z. 2011. Evaluation of a Bayesian coalescent method of species delimitation. *Systematic Biology* 60: 747–761. https://doi.org/10.1093/sysbio/syr071

Zhang J., Kapli P., Pavlidis P. & Stamatakis A. 2013. A general species delimitation method with applications to phylogenetic placements. *Bioinformatics* 29: 2869–2876. https://doi.org/10.1093/bioinformatics/btt499

Manuscript received: 20 March 2022
Manuscript accepted: 4 July 2022
Published on: 9 September 2022
Topic editor: Tony Robillard
Desk editor: Danny Eibye-Jacobsen

Printed versions of all papers are also deposited in the libraries of the institutes that are members of the *EJT* consortium: Muséum national d'histoire naturelle, Paris, France; Meise Botanic Garden, Belgium; Royal Museum for Central Africa, Tervuren, Belgium; Royal Belgian Institute of Natural Sciences, Brussels, Belgium; Natural History Museum of Denmark, Copenhagen, Denmark; Naturalis Biodiverstiy Center, Leiden, the Netherlands; Museo Nacional de Ciencias Naturales-CSIC, Madrid, Spain; Leibniz Institute for the Analysis of Biodiversity Change, Bonn – Hamburg, Germany; National Museum, Prague, Czech Republic.

Supplementary files

Suppl. file 1 (Supplementary Table 1). Primers for tested *Wolbachia* markers that did not produce a PCR product in our material.
https://doi.org/10.5852/ejt.2022.836.1921.7693

Suppl. file 2 (Supplementary Table 2). Specimens with associated genetic data.
https://doi.org/10.5852/ejt.2022.836.1921.7695

Suppl. file 3 (Supplementary Figures 1–3). Maximum likelihood trees from analysis of datasets in MEGA X.
Suppl. Fig. 1. Maximum likelihood tree from analysis of the COI-dataset in MEGA X. Bootstrap support (500 replicates) on branches.
Suppl. Fig. 2. Maximum likelihood tree from analysis of the 18S-dataset in MEGA X. Bootstrap support (500 replicates) on branches.
Suppl. Fig. 3. Maximum likelihood tree from analysis of the 28S-dataset in MEGA X. Bootstrap support (500 replicates) on branches.
https://doi.org/10.5852/ejt.2022.836.1921.7697